Title

Efficient separation of carbon dioxide and methane in high-pressure and wet gas mixtures using Zr-MOF-808

Authors

Menezes, Tamires R
Santos, Kátilla MC
Mao, Haiyan
et al.

Publication Date

2025-02-01

DOI

10.1016/j.seppur.2024.129033

Peer reviewed

Separation and Purification Technology

EFFICIENT SEPARATION OF CARBON DIOXIDE AND METHANE IN HIGH-PRESSURE AND WET GAS MIXTURES USING Zr-MOF-808

--Manuscript Draft--

Manuscript Number:	
Article Type:	Full Length Article
Section/Category:	Adsorbent synthesis (carbons, zeolites, metal organic frameworks) for gas or liquid applications
Keywords:	Metal-organic framework (MOF); MOF-808; CO2; CH4; Adsorption; high pressure
Corresponding Author:	Juliana Faccin de Conto Tiradentes University Aracaju, BRAZIL
First Author:	Tamires Reis Menezes
Order of Authors:	Tamires Reis Menezes
	Kátilla M.C. Santos
	Haiyan Mao
	Klebson Santos
	Juliana Faccin de Conto
	Jeffrey A. Reimer
	Silvia M. E. Dariva
	Cesar C. Santana
Abstract:	Due to global warming, the capture and separation of CO2 has been the focus of a plethora of research in order to mitigate its emissions and contribute to global development. Given that CO2 is commonly found in natural gas currents, there have been efforts to seek more efficient materials to separate gaseous mixtures such as CO2/CH4. However, there are only a few reports in regards to adsorption processes within pressurized systems. In the offshore scenario, natural gas currents still exhibit high moisture content, necessitating a greater understanding of processes in moist systems. In this article, a metal-organic framework synthesis based on zirconium (MOF-808) was carried out through a conventional solvothermal method and autoclave for the adsorption of CO2 and CH4 under different temperatures (45 °C to 65 °C) and pressures ranging from 50 to 100 bar. Furthermore, the adsorption of humid CO2 was evaluated using thermal analyses. The MOF-808 synthesized in autoclave showed a high surface area (1502 m2 g-1 per BET) and a high porosity volume (0.63 cm3 g-1 per DFT). As for the MOF-808 conventionally synthesized, though presenting a high crystallinity, it showed a lesser superficial area (1323 m2 g-1 per BET) and a lower volume of pores (0.51 cm3 g-1 per DFT) in relation to the one synthesized in the autoclave. Also, the MOF-808 synthesized in the autoclave showed a high capacity for CO2 adsorption at 50 bar and 45°C and had a low selectivity to capture CH4 molecules. It also exhibited a fine stability after five cycles of CO2 adsorption and desorption at 50 bar and 45 °C - as confirmed by structural post-adsorption analyses while maintaining its adsorption capacity and crystallinity. Furthermore, it can be observed that the adsorption capacity increased in a humid environment, and the adsorbent remained stable after adsorption cycles in the presence of moisture. Finally, it was possible to confirm the occurrence of physisorption processes through NMR analyses, validating the choice of mild temperatures for regeneration and contributing to the reduction of energy consumption in processing plants.
Suggested Reviewers:	Aarti Aarti Academy os Scientific and Innovative research aarti@iip.res.in
	Joaquín Coronas coronas@unizar.es

Aracaju, June 2024

Editor-in-Chief: Bart Van der Bruggen

Editor of Separation and Purification Technology

Dear Prof. Bart Van der Bruggen,

For your appreciation, we are submitting the article entitled **"EFFICIENT SEPARATION OF CARBON DIOXIDE AND METHANE IN HIGH-PRESSURE AND WET GAS MIXTURES USING Zr-MOF-808"** by Tamires Menezes, Kátilla Santos, Haiyan Mao, Klebson Santos, Juliana De Conto, Jeffrey Reimer, Silvia Dariva, Cesar C. Santana to **Separation and Purification Technology**.

Please, find below the explanation of manuscript significance.

Capture and separation of CO_2 has been the focus of a plethora of research in order to mitigate its emissions and contribute to global development. Given that CO_2 is commonly found in natural gas currents, there have been efforts to seek more efficient materials to separate gaseous mixtures such as CO_2/CH_4. However, there are only a few reports in regards to adsorption processes within pressurized systems. In the offshore scenario, natural gas currents still exhibit high moisture content, necessitating a greater understanding of processes in moist systems. The metal-organic frameworks emerge as a promising alternative since their porous structures render rather peculiar characteristics such as high porosity, selectivity, high variety of dimensions, and topologies. In this article, a metal-organic framework synthesis based on zirconium (MOF-808) was carried out through a conventional solvothermal method and autoclave for the adsorption of CO_2 and CH_4 under different temperatures (45 °C to 65 °C) and pressures ranging from 50 to 100 bar. Furthermore, the adsorption of humid CO_2 was evaluated using thermal analyses.

Thus, this paper will show that MOF-808 showed a high capacity for CO_2 adsorption at 50 bar and 45°C and had a low selectivity to capture CH_4 molecules. Furthermore, it can be observed that the adsorption capacity increased in a humid environment, and the adsorbent remained stable after adsorption cycles in the presence of moisture. Finally, it was possible to confirm the occurrence of physisorption processes through NMR analyses, validating the choice of mild temperatures for regeneration and contributing to the reduction of energy consumption in processing plants.

Our investigation is related to the encompass of Separation and Purification Technology readers and to the Journal scope. Finally, the authors state that the work was not under consideration for publication elsewhere. Moreover, all authors have approved this submission.

We hope that our manuscript accomplishes the requirements and general standards of quality of Separation and Purification Technology.

Thank you in advance,

Sincerely yours,

Prof. Juliana Faccin De Conto Borges (Corresponding Author)
Institute of Technology and Research – ITP,
Center for Studies in Colloidal Systems – NUESC,
Laboratory of Materials Synthesis and Chromatography – LSINCROM,
Av. Murilo Dantas, 300, CEP-490032-490, Aracaju-SE, Brazil
Phone: (+55) 79 3218 2164
E-mail: jfconto@gmail.com juliana_faccin@itp.org.br

Highlights

MOFs are highly porous

MOF-808 is an efficient adsorbent for CO_2 adsorption

MOF-808 are promising for separation of CO_2/CH_4 operating at high pressure

MOF-808 great stability of this material even under high pressures

Stable Performance and Selectivity: MOF-808 demonstrated stable CO_2 adsorption and low CH_4 selectivity after multiple cycles, crucial for efficient CO_2 capture

The durability of the MOF-808 adsorbent in humid environments optimizes CO_2 capture efficiency and reduces energy consumption in processing plants

EFFICIENT SEPARATION OF CARBON DIOXIDE AND METHANE IN HIGH-PRESSURE AND WET GAS MIXTURES USING Zr-MOF-808

Tamires R. Menezes[a,b], Kátilla M.C. Santos[a,b], Haiyan Mao[c], Klebson Santos[a,b], Juliana F. De Conto[a,b], Jeffrey A. Reimer[c], Silvia M. E. Dariva[a,b], Cesar C. Santana[a,b].

[a]Laboratory of Materials Synthesis and Chromatography, Institute of Technology and Research, Aracaju, SE 49032-490, Brazil

[b]Graduate Program in Process Engineering, Tiradentes University, Aracaju, SE 49032-490, Brazil

[c]Department of Chemical and Biomolecular Engineering, University of California, Berkeley, Berkeley, CA 94720, USA.

*Corresponding author: Juliana Faccin De Conto Borges

Tel: (+55) 79 3218 2164

Email: jfconto@gmail.com / juliana_faccin@itp.org.br

Abstract:

Due to global warming, the capture and separation of CO_2 has been the focus of a plethora of research in order to mitigate its emissions and contribute to global development. Given that CO_2 is commonly found in natural gas currents, there have been efforts to seek more efficient materials to separate gaseous mixtures such as CO_2/CH_4. However, there are only a few reports in regards to adsorption processes within pressurized systems. In the offshore scenario, natural gas currents still exhibit high moisture content, necessitating a greater understanding of processes in moist systems. In this article, a metal-organic framework synthesis based on zirconium (MOF-808) was carried out through a conventional solvothermal method and autoclave for the adsorption of CO_2 and CH_4 under different temperatures (45 °C to 65 °C) and pressures ranging from 50 to 100 bar. Furthermore, the adsorption of humid CO_2 was evaluated using thermal analyses. The MOF-808 synthesized in autoclave showed a high surface area (1502 $m^2\ g^{-1}$ per BET) and a high porosity volume (0.63 $cm^3\ g^{-1}$ per DFT). As for the MOF-808 conventionally synthesized, though presenting a high crystallinity, it showed a lesser superficial area (1323 $m^2\ g^{-1}$ per BET) and a lower volume of pores (0.51 $cm^3\ g^{-1}$ per DFT) in relation to the one synthesized in the autoclave. Also, the MOF-808 synthesized in the autoclave showed a high capacity for CO_2 adsorption at 50 bar and 45°C and had a low selectivity to capture CH_4 molecules. It also exhibited a fine stability after five cycles of CO_2 adsorption and desorption at 50 bar and 45 °C - as confirmed by structural post-adsorption analyses while maintaining its adsorption capacity and crystallinity. Furthermore, it can be observed that the adsorption capacity increased in a humid environment, and the adsorbent remained stable after adsorption cycles in the presence of moisture. Finally, it was possible to confirm the occurrence of physisorption processes through NMR analyses, validating the choice of mild temperatures for regeneration and contributing to the reduction of energy consumption in processing plants.

Keywords: Metal-organic framework (MOF); MOF-808; CO_2; CH_4; Adsorption; high pressure.

1. Introduction

Carbon dioxide (CO_2), one of the leading causes of global warming, is also one of the most abundant components in the fossil fuel combustion process and is commonly found in natural gas streams [1]. Within the last few years, many oil and gas reservoirs have been discovered in countries such as Malaysia, Indonesia, and Brazil - all with CO_2 grades of up to 80 % [2,3].

In the offshore reservoir's scenario, in addition to CO_2, there is a presence of high-water content, which, depending on the pressure and temperature conditions, favors the formation of acidic environments, causing corrosion in equipment and complicating both compression and fuel transportation [4,5]. Therefore, the need arises to capture and store carbon (CCS) directly on the platforms, preventing their emission into the atmosphere and contributing to the global effort to reduce CO_2 levels.

Out of the processes that focus on the removal of CO_2 from NG currents, those of absorption and adsorption are highlighted. Although these conventional techniques are vastly employed with the use of different materials based on amines [6], modified silica [7], and zeolites [8,9], they come with some challenges including high energy expenditure, formation of toxic and volatile compounds for the environment, and a non-efficacious removal of contaminants. Therefore, several efforts have been employed to search for materials that are more efficient in the removal of CO_2 - mostly with an emphasis on the separation of CO_2 and CH_4 [10–13].

In the context of CO_2 removal in NG currents (and post-combustion processes), it is crucial to consider essential properties such as moisture resistance, ease of regeneration, and thermal stability. This is because CO_2 is typically present in gas streams containing significant moisture. One of the most widely used adsorbents in industry today is Zeolite 13X, which has a strong affinity for water. Yet in processes involving moist gases, the CO_2 adsorption capacity of this

adsorbent decreases, thus high temperatures are required for its regeneration, leading to high energy consumption in processing plants. Considered a promising alternative, highly porous metal-organic frameworks (MOFs) have been the focus of attention due to their selectivity, high adsorptive capacity and ease of regeneration under milder temperatures, below 140 °C, which results in lower energy expenditure for e.g., natural gas processing plants [3,14,15]. These are hybrid materials that combine inorganic components (clusters) with organic components (linkers) to form highly porous three-dimensional crystalline structures [16,17].

These materials have been greatly used towards separation [18,19], storage [20,21], and gasses purification [22–24]. As for the separation of CO_2/CH_4, several MOFs with different metallic sites have been reported, such as aluminum [21,25], zirconium, copper [26,27], and zinc [28]. As such, they have promising characteristics for CO_2/CH_4 separation due to their high selectivity arising from the metallic sites with the organic linkers. These structures are reported with or without modifications, as well as in the form of membranes and films [29–31].

The excellent performance in the separation of binary mixtures such as CO_2/CH_4, CO_2/N_2, and CO_2/O_2 is linked to the outstanding surface areas of these structures, as well as their high pore volumes, unique pore topologies, and the presence of numerous coordinatively unsaturated sites (CUSs). Most studies on these binary mixture separations occur under dry conditions, where MOFs exhibit excellent selectivity results. However, the performance in processes under humid conditions often cannot be sustained due to instability in the presence of water. In many situations, this instability is associated with the degradation of the structure due to slow hydrolysis when exposed to humid conditions, as observed in MOFs like HKUST-1 [32,33], MOF-5 [34–36], MOF-3 and MOF-74 [37]. However, in the literature, various metal-organic frameworks are found to demonstrate stability in the presence of water, thanks to a robust metal cluster. Some notable

examples include Al-MIL [38–40], Cr-MIL [41,42], UiO [38,43] and Zr-MOF [44–46], which exhibit strong resistance to moisture and excellent thermal stability.

Metal-organic frameworks based on zirconium have been well investigated mainly due to their excellent stability in comparison to CO_2 and water. Out of these metal-organic frameworks based on Zr, the MOF-808 have gained significant attention. This structure, as noted in studies such as [47–49], shows proper stability and high adsorptive capacity in relation to CO_2 - besides being regenerated under milder temperatures between 80 °C e 150 °C.

However, in general, CO_2 and CH_4 adsorption studies with metal-organic frameworks are reported with pressures of up to 1 bar [47,50,51]. There are only a few contributions in the literature about CO_2 and CH_4 under pressurized systems with these materials [44,52,53]. Furthermore, there is a few studies on the use of metal-organic frameworks in situations involving humid environments. Thus, in this article, CO_2 and CH_4 adsorption were measured at high pressure (up to 100 bar) with different temperatures using a metal-organic framework based on zirconium (MOF-808), aiming to contribute to studies of real parameters as applied to industrial processing plants working with the mixture of both gasses.

2. Experimental

2.1. Conventional solvothermal synthesis of MOF-808

The MOF-808 structure was adapted from [54] and [55]. In a synthesis vial containing 0.11 g of trimesic acid (H3BTC - 95 %-Sigma-Aldrich) and 0.16 g of zirconium chloride (ZrOCl2.8H2O - 98 %-Sigma-Aldrich) were added to 20 ml of N,N-dimethylformamide (DMF) ($HCON(CH_3)_2$ – 99.8 % Sigma-Aldrich) and 20 ml of formic acid (HCOOH - 95 %-Sigma-Aldrich). The mixture was heated up in a convection oven under 100 °C for 7 days, after that, the crystals were filtered and washed 3 times with 10 ml of anhydrous DMF (99.8 % Sigma-Aldrich).

The solids were then immersed in 10 ml of acetone (CH3COCH3 – 99.5 % Sigma-Aldrich) for 3 days, with the latter being changed 3 times daily. Lastly, they were filtered and dried under 150 °C. This material was named MOF-808-C.

2.2. Solvothermal synthesis in the MOF-808 autoclave

The MOF-808 synthesis through autoclave was adapted from [56], in order to obtain a metal-organic framework as efficient as the conventional one, so to accelerate the process of obtaining the material and thus lowering energy expenditure. In a teflon cup, 0.315 g of trimesic acid (H3BTC) and 0.727 g of zirconium chloride (ZrOCl2.8H2O) were added to 33.7 ml of DMF and 33.7 ml of formic acid. An ultrasonic bath was used for 5 min, and the mixture was placed in an autoclave, and kept under 130 °C for 48 hrs. The solution was filtered, and the white precipitate was washed 3 times with 30 ml DMF. After that, the material was washed with 30 ml of deionized water 3 times and, finally, washed with 30 ml of acetone 3 more times. Afterwards, the crystals were dried in the convection oven under 150 °C for 24 hrs. This material was named MOF-808-AC.

2.3. Characterization

N_2 adsorption-desorption isotherms at 77 K were measured using a NOVA 1200e-Surface Area and Pore Size Analyzer, Quantachrome Instruments-version 11.0. The samples were degassed at 130 °C for 6 h before the adsorption measurements. The surface area was calculated by the Brunauer–Emmett–Teller (BET) model and the total pore volume by the DFT (density functional theory) and HK (Horvath-Kawazoe) models. XRD analyses were performed using a Rigaku Miniflex II diffractometer equipped with Cu ($\lambda = 1.54$) source radiation, in the range of $2° < \theta < 30°$, operated at 40 kV and 40 mA. Thermogravimetric analysis was performed using a HITACHI model STA7200RV thermal analyzer under a nitrogen flow of 150 ml min^{-1}. The

samples were heated from 25 to 950 °C in an alumina sample holder under a constant heating ratio of 10 °C min^{-1}.

Fourier-transform infrared spectroscopy (FTIR) analyses were measured on attenuated total reflectance (ATR) spectrophotometer (BRUKER). The resolution adopted was 2 cm^{-1}, and 32 min^{-1} scans. Scanning electron microscopy SEM analysis was performed using a JEOL JSM-IT200 scanning electron microscope with beam acceleration at 20 kV and current at 60 uA (probe current). SEM images were processed with a Python algorithm based on the scikit image library [57]. This algorithm was used to measure the properties of each particle, including its size and sphericity.

2.4. Measurements of CH_4 and CO_2 adsorption

CO_2 adsorption (White Martins - 99.5%) was conducted at temperatures of 45 °C, 55 °C, and 65 °C, at pressures up to 50 bar. For CH_4 adsorption (White Martins - 99.5 %), a temperature of 45 °C and pressures up to 100 bar were used. The analyses were performed using a high-pressure gas adsorption instrument (Isorb-HP1 - Quantachrome), to which a syringe pump (ISCO, model 260D) was attached. The selected experimental conditions aim to simulate industry-standard conditions. For the analyses, an empty column adsorption curve was initially obtained to determine the cell volume without the sample. Subsequently, approximately 200 mg of the sample was degassed to ensure the removal of moisture and to make the pores accessible for adsorption. The degassing conditions were as follows: 30 min at 50 °C, 30 min at 80 °C, and 4 hours at 130 °C, under vacuum.

2.5. Adsorption-desorption cycles of CO_2 adsorption

Six cycles of CO_2 adsorption-desorption were conducted to assess the material's stability under high pressure. Firstly, a degassing process was performed on the sample to remove possible

moisture. The degassing conditions were as follows: 30 min at 50 °C, 30 min at 80 °C, and 4 hours at 130 °C. For the adsorption analyses, approximately 200 mg of the sample were used, and adsorption took place at 45 °C and 50 bar. Regeneration was carried out under PSA until a vacuum was achieved, and the sample was maintained under vacuum for 30 min.

2.6. Thermodynamic parameters

The values of the thermodynamic parameters of enthalpy (ΔH) and entropy (ΔS) were calculated using the high-pressure isotherms software isorbHPwin with the PCT (pressure, concentration, and temperature) graph of CO_2 adsorption data. With the enthalpy (ΔH) and entropy (ΔS) results and using the thermodynamic relationship present in (Equation 1), it was possible to calculate the Gibbs Free Energy.

$$\Delta G_{ads}^{0} = \Delta H_{ads}^{0} - T\,\Delta S_{ads}^{0} \quad (1)$$

2.7. Adsorption models

The Toth model (Equation 2), an empirical model developed to combine the characteristics of the Freundlich and Langmuir models [58], was applied to the CO_2 adsorption isotherms on the MOF-808-AC, which is widely used in metal-organic frameworks.

$$q_i = q_{m,i}\frac{K_i * P}{[1+(K_i * P)^{n_i}]^{\frac{1}{n_i}}} \quad (2)$$

The parameters of this equation correspond to: q_i = adsorbed quantity; $q_{m,i}$ = maximum adsorption capacity of component i; n_i = characterizes the heterogeneity of the adsorption system (if n = 1, the system is homogeneous); P = pressure; K_i = interactions between adsorbent-adsorbate (if K_i tends to low values and q_m to high values, the model becomes closer to a linear isotherm).

2.8. Humid Thermogravimetric analysis

Thermogravimetric analysis (TGA) humid was performed using a TA Instruments TGA Q50. The samples were activated under N_2 flowing at 130 °C until stabilization mass, around 30 min. Then, the gas was conducted through water bubblers, with an estimated water content of ~ 30 % R.H at room temperature. For the adsorption and desorption analysis was used a ramp rate of 1 °C min^{-1}.

2.8. CO2 gas dosing to NMR measurement

A 4 mm rotor was packed with previously activated samples. The CO_2 dosage was performed at room temperature up to 1000 mbar and was adjusted with a capacitance manometer (model 722B, MKS Instruments). To begin, a vacuum was created throughout the line to remove any potential moisture. To ensure sample saturation, $^{13}CO_2$ gas (99 atomic% 13C; Sigma-Aldrich) was dosed for 2 hours. All of the above methodology was repeated for the samples dosed with CO_2 and water, and water was added to the system.

2.9. NMR measurement

Solid-state NMR experiments were performed using Bruker AV-500 equipment with an Avance I console (magnetic field strength of 11.7 T) operating at resonance frequencies of 500.12 MHz for ^{1}H, and 125.72 MHz for ^{13}C. Equipped with a 4 mm $^{1}H/^{13}C$ High-Resolution Magic Angle Spinning probe (HR-MAS) with a magic angle gradient and a 4 mm 1H/BB CP-MAS probe. The sample spinning rate of 10 kHz for all the experiments. The acquisition time for 13C experiments was conducted at a recycle delay of 2 s and the spectral window ~25 to 70 kHz, with a contact time of 2 ms.

3. Results and Discussion

3.1. Characterization of the metal-organic frameworks MOF-808-C and MOF-808-AC

Intense peaks can be noted from x-ray diffraction, Figure 1, which causes high MOF-808 crystallinity. Their characteristic Bragg peaks are in accordance with studies reported in literature [59–62] and the simulated theoretical standard was obtained from the Cambridge Crystallographic Data Centre (ICSD), code CCDC 1509776. The samples have similar diffraction peak shapes without amorphous phases and no diffraction peaks of impurities were detected. The crystalline peaks (8.35°), (8.75°), (10.0°) and (11.0°) are related to the crystalline framework of planes (311), (222), (400), and (331) respectively - thus rendering the synthesis of both MOF-808-C and MOF-808-AC metal-organic frameworks successful [63,64]. It is noteworthy that regardless of having less time to perform the synthesis in the autoclave, the MOF structural standard was maintained.

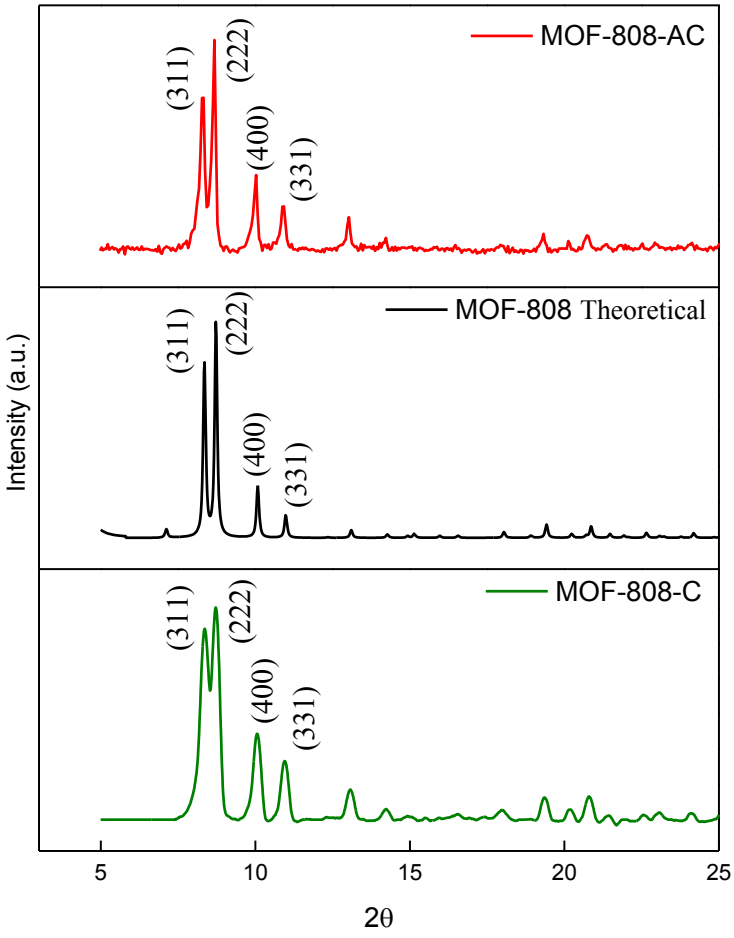

Figure 1. Experimental and theoretical X-ray diffraction profiles of the MOF-808-C (a) e MOF-808-AC (b).

In the N_2 adsorption analysis, Figure 2, it can be noted that both materials showed Type I isotherms, characteristics of microporous materials (XUAN et al. 2019 and GU et al. 2020). Further, a high superficial surface area by BET is noted, 1502 $m^2\ g^{-1}$ for MOF-808-AC and a smaller area of 1323 $m^2\ g^{-1}$ for MOF-808-C. As well as high values of pore volumes, 0.63 $cm^3\ g^{-1}$ for the MOF-808-AC and 0.51 $cm^3\ g^{-1}$ for the MOF-808-C as calculated via DFT. These values are in accordance with the ones reported by LIN et al. 2019, XUAN et al. 2019 and ZHANG et at.

2013, where the area for this MOF is around 1600 m^2 g^{-1} per BET and 0.64 cm^3 g^{-1} per DFT [4,59,60,64].

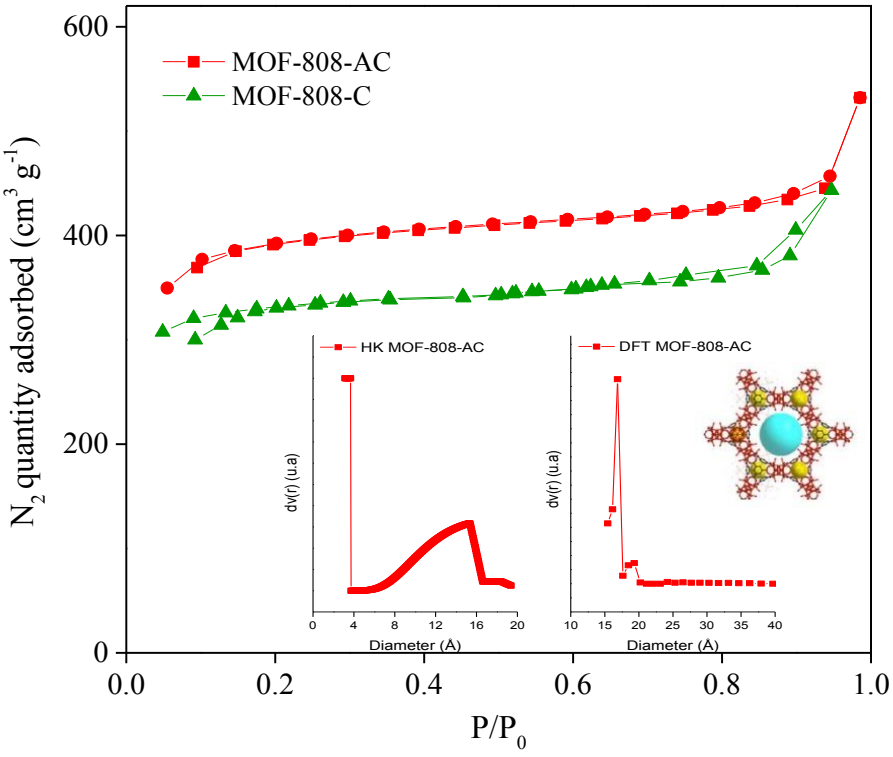

Figure 2. N_2 adsorption/desorption isotherms at 77K of samples MOF-808-AC and MOF-808-C. Pore diameter distribution was calculated by HK and DFT.

In the size distribution of the HK model pores, Figure 2, it was possible to note the presence of micropores near 4 Å, which relates to the narrowest micropores, in accordance with the literature that reports smaller pores near 4 Å formed by the Zr and the BTC ligand [65]. The pore size distribution graph of the DFT model shows pores of 17 Å - 19 Å for MOF-808-AC this may be indicative of the presence of remaining solvent in the MOF-808 pores, which will be better discussed in later analyses. In the literature, the MOF-808 has a central cavity around 18 Å, that is

formed in the midst of tetrahedral cages [65]. The discrepancy between the areas observed in the literature and in this study, as well as the results presented in size distribution pores, may suggest the presence of residues in the pores of MOF-808, which will be examined in more detail later on.

Thermogravimetric analyses were carried out as seen in Figure 3. It is noted that in both samples there are three stages of mass variation, thus corroborating what has been reported by CIRUJANO et al. 2020 [63] and WANG et al. 2022 [38]. The first stage, between 25 °C and 120 °C may be attributed to the desorption of physisorbed water molecules or reminiscent solvents adsorbed on the surface sample [66] - representing less than 10 % for the MOF-808-C and around 20 % for the MOF-808-AC. The second stage, 10 % variation were noted for the MOF-808-AC and 13 % MOF-808-C, between 180 °C and 370 °C, as a result of the decomposition of formic acid as coordinated with the Zr_6 [59,67]. Such a presence of the formic acid on the pores may justify the difference between the surfaces of both samples as previously shown in Figure 2, as well as the presence of narrow pores, evidencing a greater quantity of formic acid remaining on the pores of the MOF-808-C and a low efficiency on the washing of the material, as it was done to change the solvent, differently than the filtration under vacuum performed at the MOF-808-AC.

In the last stage, around 500 °C, the main mass variation takes place with the decomposition of the organic part (BTC), thus indicating the collapse of these groups with only the zirconium oxide - ZrO_2 remaining. Hence, it is possible to identify through this analysis that both structures are thermally stable at up to approximately 400 °C [59,68,69]. It gives grounds for the possibility of utilizing milder temperatures, under 150 °C, thus allowing for the removal of impurities from the pores of these metal-organic frameworks. It may contribute to reducing energy expenditure at industrial processing plants.

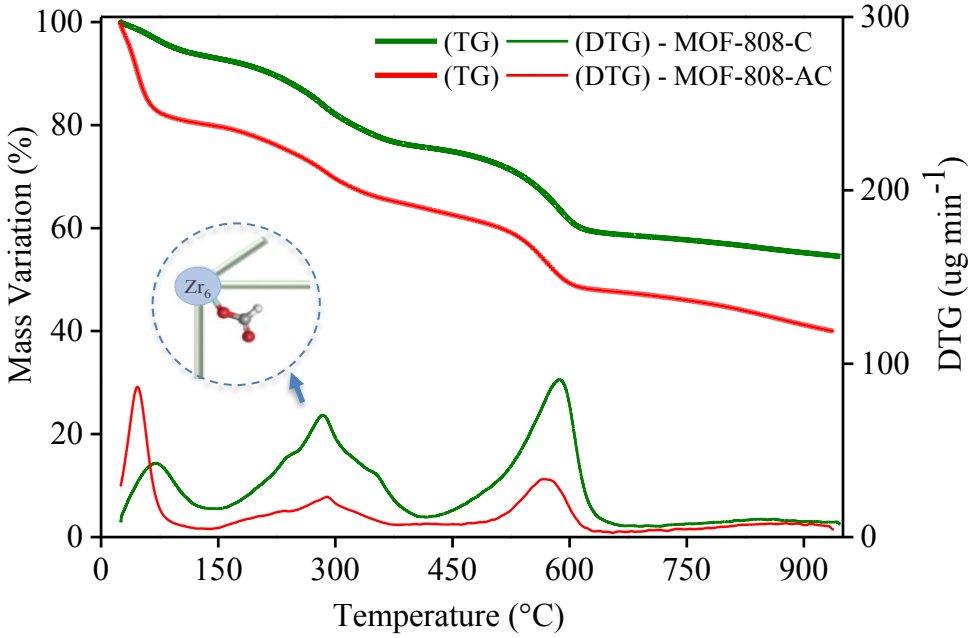

Figure 3. TG-DTG curves of MOF-808 metal-organic framework obtained at a heating rate of 10 °C min^{-1} in a dynamic N_2 atmosphere (150 ml min^{-1}).

In Table 1, the CHN elementary analysis data is shown for the MOF-808-C and the MOF-808-AC. Carbon percentages of 20.27 % were found for the MOF-808-AC and 21.06 % for MOF-808-C, while the hydrogen percentage was 2.86 % and 2.47 %, respectively. The greater percentage of carbon present in the MOF-808-C is directly related to the presence of formic acid within the pores of this sample – as observed in the TGA analyses.

Table 1. Elemental analysis triplicate mean (CHN) of samples MOF-808-C and MOF-808-AC.

Samples	% C	% H
MOF-808-AC	20.27	2.86
MOF-808-C	21.06	2.47
[70]	20.36	2.81
Theoretical	20.36	2.81

Through the scanning electron microscopy, as seen in Figure 4, it is noted that both samples have particle conglomerates of monodisperse morphologies and that are evenly distributed, with octahedral microcrystals, as observed by JIANG et al. 2014, LIU et al. 2019 and LOGAN et al. 2020 [59,62,71]. An algorithm programmed in Python 3.7 from the sciki image library was used in order to examine the circularity of the particles as well as their equivalent diameters.

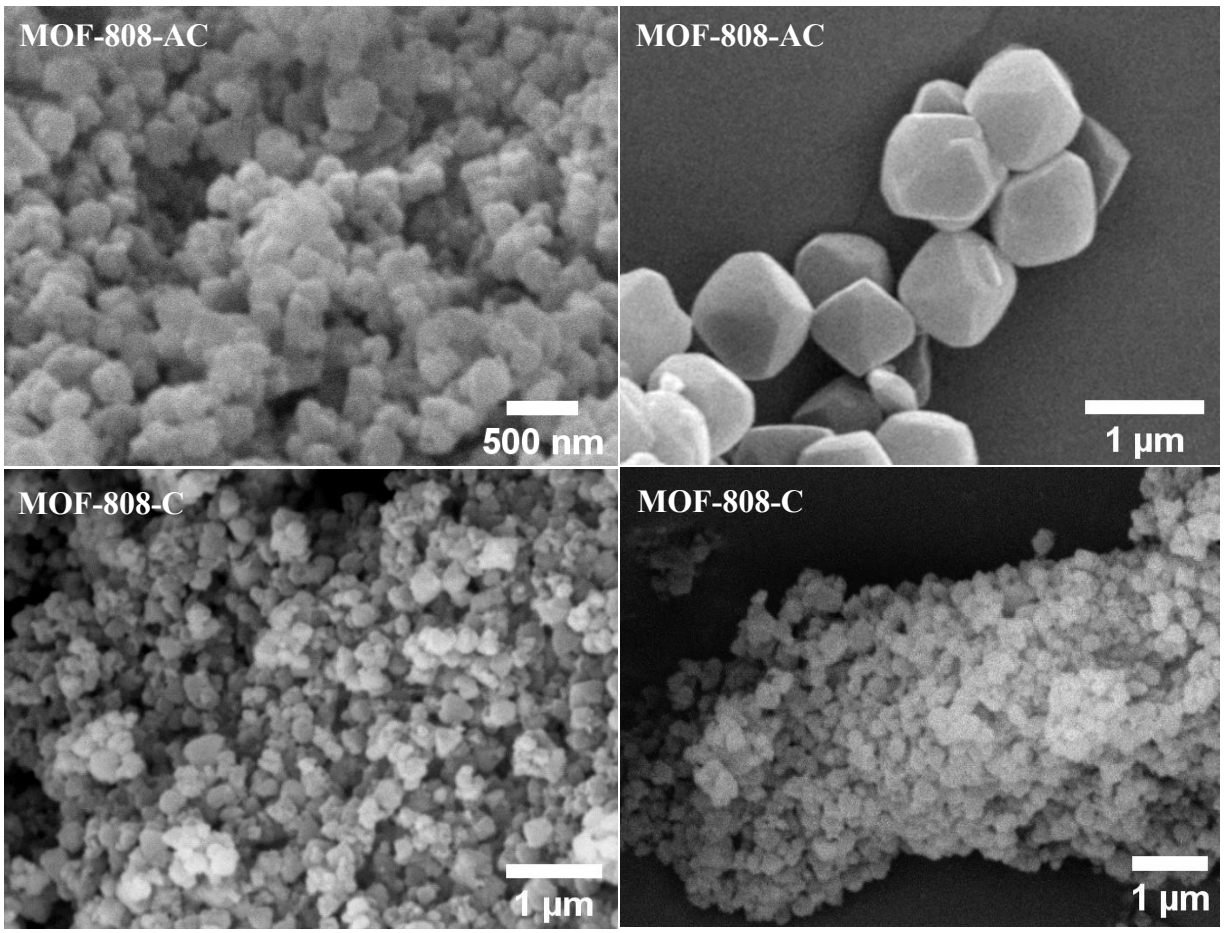

Figure 4. Scanning Electron Microscopy of the metal-organic frameworks MOF-808-AC and MOF-808-C: a) at 30,000 magnifications; b) 25,000 magnifications; c) 20,000 magnifications; d)16,000 magnifications.

Figure 5 shows the particles identified and measured by the algorithm for both the MOF-808-C and the MOF-808-AC samples. It is seen in Figure 6 that the particles have an equivalent diameter at the 0.2 µm - 0.4 µm bandwidth, 64 % for MOF-808-C and 78 % for the MOF-808-AC. In the literature, the MOF-808 is close to 0.2 µm in size, thus indicating that a value above 0.2 µm is related to the presence of agglomerates. Furthermore, in Figure 6, it is noted that the circularity of the particles is between bandwidths 0.6 and 1 – according to the theoretical value of the sphericity of the octahedron, 0.846 [69].

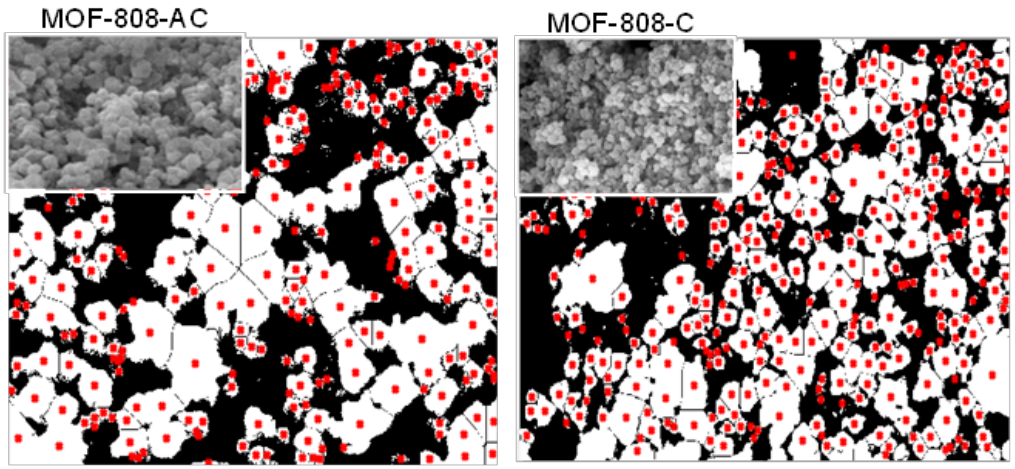

Figure 5. Detection of MOF-808-C and MOF-808-AC particles by Python 3.7 from the sciki image library.

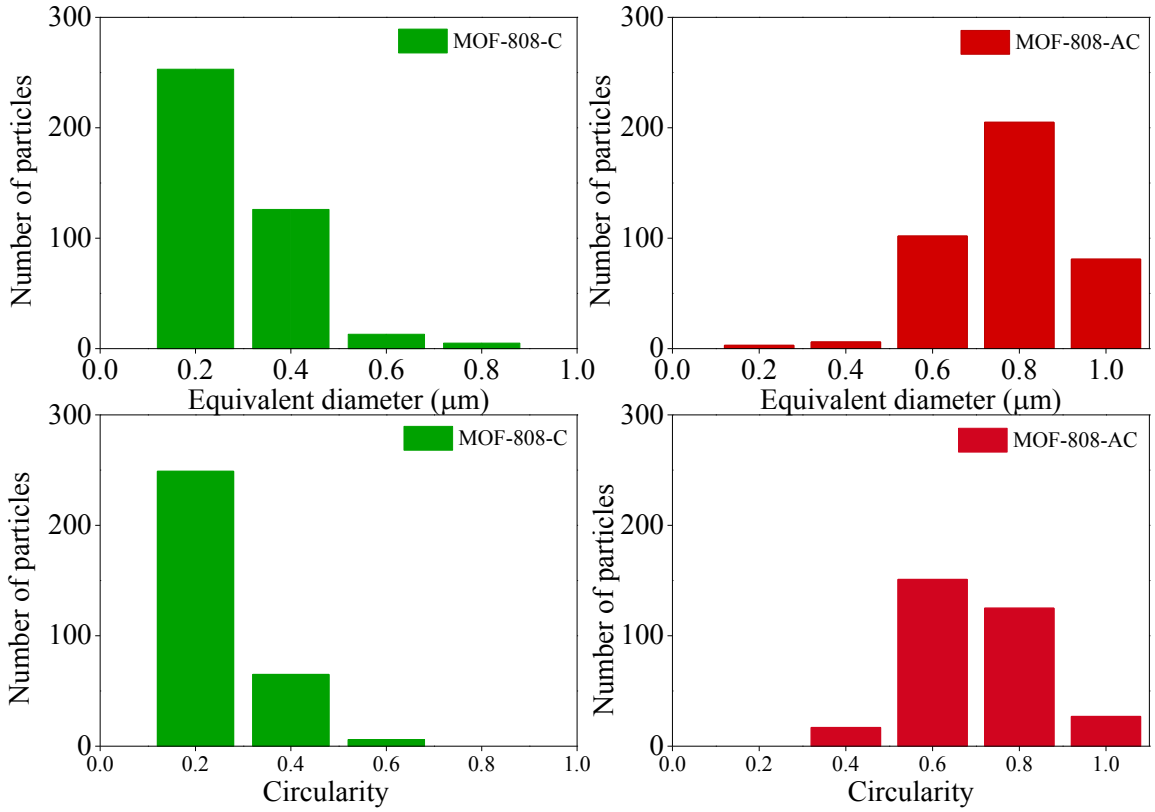

Figure 6. Equivalent diameter and circularity obtained from Python for samples: MOF-808-AC and MOF-808-C.

Figure 7 shows the FTIR analysis for MOF-808-C and MOF-808-AC. The 1606 cm^{-1}, 1583 cm^{-1} and 1446 cm^{-1} vibration bands are attributed to asymmetrical and symmetrical stretching vibrations of the BTC carboxyl groups (−COOH) which are adsorbed physically within the given structure [69,72,73]. As for the Zr-OH groups, they caused the absorption bands to be at 1381 cm^{-1}. The adsorption bands at 759 cm^{-1}, 710 cm^{-1} and 656 cm^{-1} are characteristics of the Zr-O vibration, which is highlighted at the band at 646 cm^{-1} - therefore corroborating the coordination reaction between the carboxyl in the BTC groups and the zirconium ion [38,67,73]. Worth noting is that just as the x-ray diffraction analysis (regardless of its route), both samples have similar structural aspects.

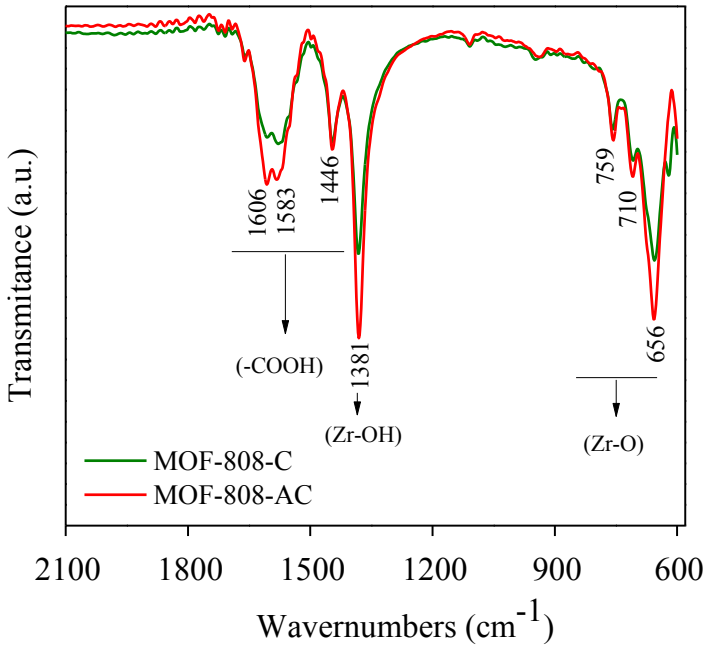

Figure 7. Infrared spectrum (FTIR) of the metal-organic frameworks MOF-808-C and MOF-808-AC.

As shown in physicochemical characterizations, the MOF-808 synthesized in the autoclave showed a better superficial area, greater volume of pores, and maintained the structural characteristics of crystallinity with a reduction in the preparation timing as compared to the

conventionally synthesized one. For this reason, this MOF-808-AC sample was chosen to be applied in the adsorption of CO_2 and CH_4.

3.2. Measurements of CO_2 and CH_4 adsorption

3.2.1. CO_2 adsorption

The CO_2 adsorption isotherms for the MOF-808-AC structure are represented in Figure 8 with the following conditions: temperatures of 45 °C, 55 °C and 65 °C under a pressure range between 1 to 50 bar. It is worthy to note that the sample did not reach its highest adsorption capacity in none of the conditions studied.

The presence of micropores in this structure eases the emergence of electrostatic interactions between the metal-organic framework and the CO_2 molecules, which favors the potential adsorption [74]. Also, the presence of narrower micropores in the MOF-808-AC (~ 4.8 Å or 0.48 nm) may function in a more selective and likely way to adsorb more CO_2. According to LU et al. (2011), one of the desirable characteristics to increase the CO_2 adsorption capacity is the proper size of the pores and their compatibility with the kinetic diameter of CO_2 molecule (~ 3.3 Å), aside from the interactions between the metal-organic framework and CO_2 [75].

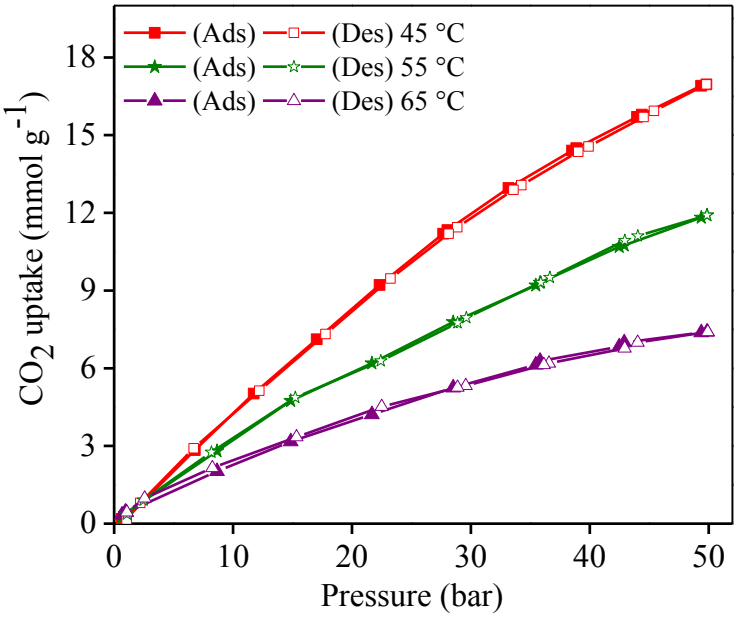

Figure 8. CO_2 adsorption isotherms of the MOF-808-AC under a pressure range between 1 and 50 bar at temperatures of 45 °C, 55 °C and 65 °C.

Hysteresis was not observed, which entails physisorption processes, reversible ones, and without capillary condensation. Consequently, a greater amount of CO_2 was adsorbed under lower temperatures – roughly 17 mmol g^{-1} under 45 °C and 50 bar. As temperature increases, there are changes in the energetic properties of molecules. In the case of CO_2, since the interaction is a Van der Walls type, the rising in temperature lowers the amount adsorbed, which is in conformity with the studies by GUAN et al. (2018), GRANDE et al. (2020) and CECILIA et al. (2020) [76–78]. Also, greater temperatures favor gaseous molecules in the free gaseous state rather than in the adsorbed one and the temperature has a direct impact on the molecular interaction between the adsorbent and adsorbate. This high amount of adsorbed CO_2 corroborates the textural properties of MOF-808 such as high porosity and accessible pores.

Table 2 represents the adsorbed CO_2 amount in the MOF-808-AC under different pressures and temperatures – as compared to the conventional adsorbents in the literature (zeolites and silicas). Where the high adsorption capacity of MOF-808 against different materials is evidenced. The adsorbent synthesized in this study has an adsorption capacity three times higher than that of most commercial materials, for example, at 40 bar, the adsorbent synthesized in this study adsorbs 14 mmol g^{-1}, whereas zeolite (NaA zeolite) adsorbs 4.5 mmol g^{-1}.

Table 2. A bibliographic survey of the amount of CO_2 adsorbed on different materials, pressure, and temperature.

Adsorbent	**Pressure / Temp** (bar) / (°C)	**Q_{ads} of CO_2** (mmol g^{-1})	**Reference**
zeolite 13X	20 / 45	6	[79]
β-zeolite	20 / 45	3.3	[80]
MOF-808-AC	20 / 45	8.2	This work
zeolite 13X	20 / 55	5	[79]
Norit R1	30 /25	10	[81]
A5 zeolite	30 / 25	2.5	[82]
RM 8852	40 / 20	3.5	[83]
NaA zeolite	40 / 30	4.5	[84]
MOF-74	42 / 25	10	[85]
Norit RB2	42 / 25	9	[85]
MOF-808-AC	40 / 45	14.5	This work
S1 coal	50 / 27	1.2	[86]
S1 coal	50 / 55	0.98	[86]
MOF-808-AC	50 / 55	11.9	This work

3.2.2. CH_4 adsorption

The isotherms in Figure 9 clearly show the greater capacity of CO_2 adsorption in comparison to that of CH_4, regardless of both being apolar and having similar kinetic diameters of 3.3 Å for CO_2 and 3.8 Å for CH_4. It probably occurs because the quadrupole moment and polarizability of the CO_2 in comparison to CH_4, promotes a greater electrostatic interaction with the open metallic sites (Zr) of MOF-808-AC [87,88]. Also, the MOF-808 features narrow pores of approximately 4 Å, acting as selectors for smaller CO_2 molecules and hindering the permeation of larger CH_4 molecules. Therefore, a low selectivity of the metal-organic framework for methane is noted – even under pure gas conditions. This means that the synthesized structure reported in this article is highly promising for the selective separation of the CO_2/CH_4 gaseous mixture.

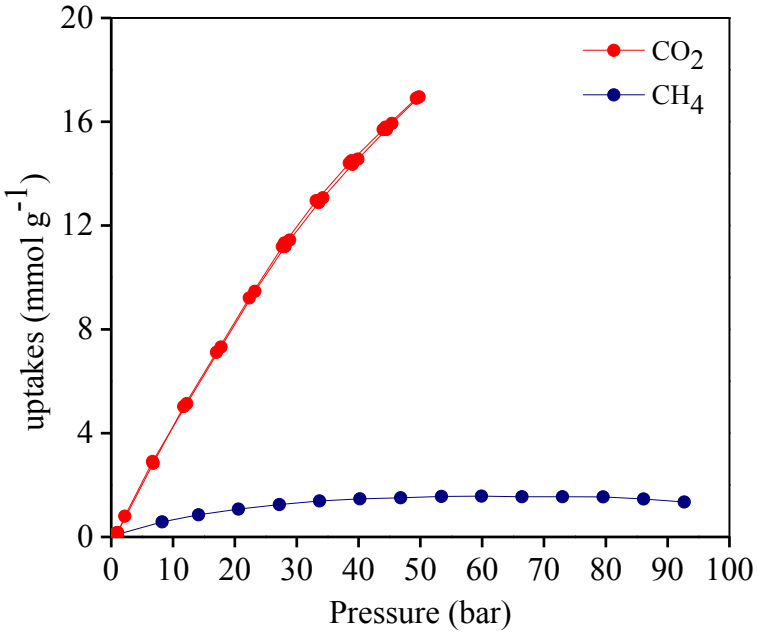

Figure 9. Adsorption isotherms of CO_2 and CH_4 on the MOF-808-AC metal-organic framework at 45 °C and up to 100 bar.

3.3. Thermodynamic parameters

The calculated values of enthalpy, entropy, and Gibbs free energy, together with the respective values of CO_2 concentration, pressure, and temperature, are presented in Table 3 for MOF-808-AC.

Table 3. Calculated thermodynamic parameters for the MOF-808-AC metal-organic framework.

CO_2 uptake (% w)	**ΔH** (kJ mol^{-1})	**ΔS** (kJ mol^{-1} k^{-1})	**Temperature** (°C)	**Pressure** (bar)	**ΔG** (kJ mol^{-1})
5	-6.0	-28.2	45	2.91	-8.97
			55	3.81	-9.26
			65	3.31	-9.54
15	-23.8	-92.2	45	7.74	-29.30
			55	12.18	-30.22
			65	13.11	-31.14
25	-33.0	-125.2	45	12.82	-39.81
			55	21.22	-41.07
			65	26.75	-42.32
35	-40.3	-163.4	45	17.96	-51.95
			55	30.97	-53.58
			65	48.38	-55.21

In Table 3, it is seen that the enthalpy values (ΔH) ranged from - 6 kJ mol^{-1} to - 40 kJ mol^{-1} for the MOF-808-AC, thus confirming that the adsorption of the CO_2 molecules in the metal-organic framework is characterized as a physisorption process. The values are in accordance with those reported in the literature, the physisorption process occurs at up to -40 kJ mol^{-1} [89,90]. Furthermore, this physisorption process is exothermic, as indicated by the negative enthalpy values. It is observable that as the quantity of CO_2 increases, the enthalpy values also rise, signifying a stronger attachment of the molecules to the surface. Nonetheless, there is no formation of chemical bonds involved in this phenomenon. The ΔG negative values indicate that the adsorption process occurs spontaneously. The ΔS negative values are a consequence of the adsorption process that lowers the level of disorder of CO_2 molecules from the moment they are

adsorbed at the active sites from the metal-organic framework – thus corroborating what was observed by PENCHAH et al. (2022) and LEE et al. (2021) [91,92].

It's noteworthy that the enthalpy associated with MOF-808 exhibits relatively low values in comparison to numerous commercially available adsorbents, including zeolites and some microporous carbons. This characteristic potentially confers a distinct advantage to the utilization of this material in cyclic separation processes, as it anticipates a reduced energy demand for adsorbent regeneration, particularly in contrast to zeolites and silicas.

3.4. Adsorption models

The experimental data for the CO_2 adsorption isotherms at 45 °C, 55 °C and 65 °C and the curves that represent the adjustments by the Toth model are presented in Figure 10. It is seen that the model presented adequate conformity with the experimental basis of the MOF-808-AC.

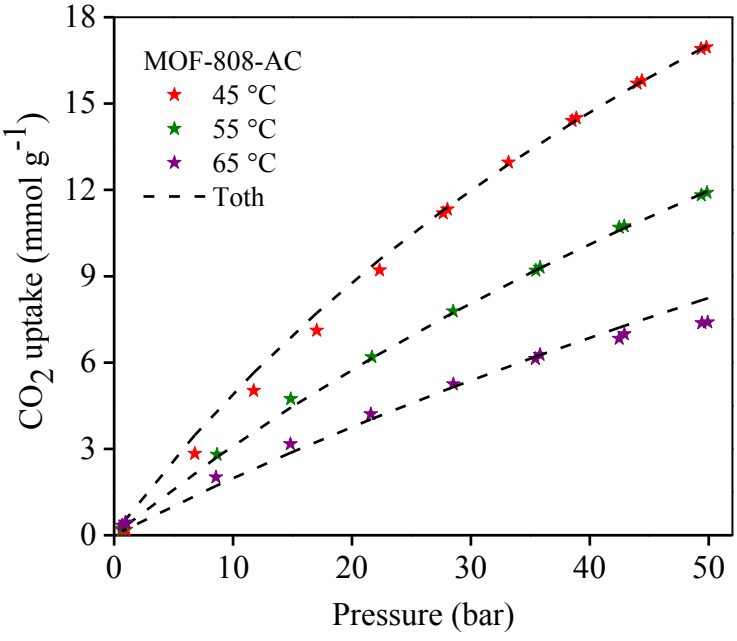

Figure 10. Adjustments of CO_2 adsorption isotherms at 45 °C, 55 °C and 65 °C between 1 and 50 bar for the MOF-808-AC. Dashed lines represent Toth's model.

The parameters obtained from the adjustment of the Toth model for the MOF-808-AC metal-organic framework are shown in Table 4. The enthalpy values calculated from the adjustment of the Toth model are in accordance with the ones previously reported. A value of - 44 kJ mol^{-1} is noted for the MOF-808-AC thus proving the process of physisorption [48,78].

Table 4. Toth model parameters for CO_2 adsorption equilibrium isotherm in metal-organic framework MOF-808-AC.

Sample	$\mathbf{q_{sat}}$ (mmol g^{-1})	**b** (bar^{-1})	$\mathbf{n_i}$	**(ΔH)** (kJ mol^{-1})
MOF-808-AC	48.7	4.5×10^{-10}	0.94	- 44.14

It may be inferred from the parameter n (0.94 for the MOF-808-AC) that the MOF-808-AC shows a heterogeneity for the CO_2 adsorption sites, since the n value was different than 1 – the value indicated in the literature by AYAWEI et al. (2017) [93]. As for the value for parameter b, it is related to the energy interaction between adsorbent and adsorbate, which shows the physisorption process applying towards both metal-organic frameworks [94].

3.5. Adsorption and Desorption cycles

Six cycles of CO_2 adsorption and desorption performed at 50 bar and 45 °C are presented in Figure 11 in order to evaluate the stability and the regeneration capacity of the MOF-808-AC. It showed a lower value between the first and the second cycle, while the others showed uniformity. This result may be due to the pores in the MOF-808 metal-organic framework being quite narrowed (~ 4.8 Å or 0.48 nm) and near the kinetic CO_2 diameter (3.3 Å for CO_2) which could have had a rupture due to the sudden pressure pumped, given that from the second cycle on there

is the pumping of 50 bar that is different from the first cycle, where a gradual pressure increase takes place for the acquisition of the isotherm as shown in Figure 8.

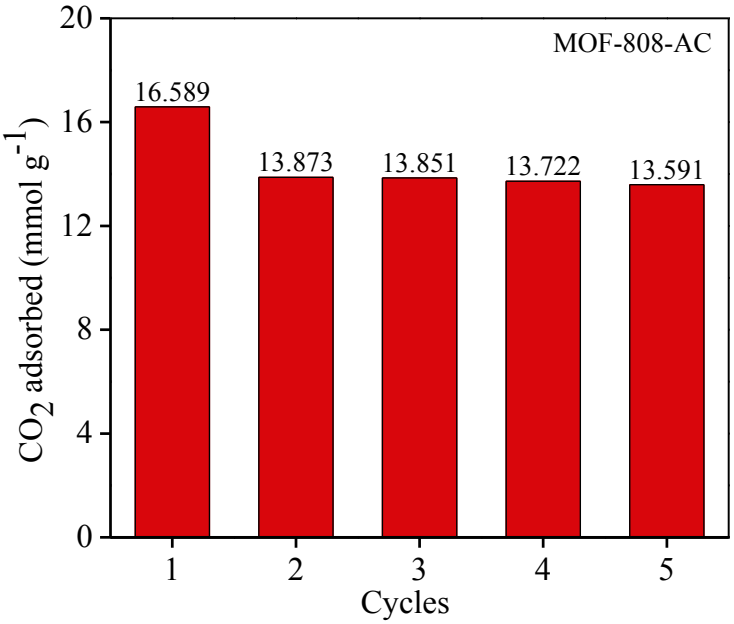

Figure 11. Adsorption and desorption cycles and adsorbed amount of CO_2 for the MOF-808-AC metal-organic framework at the temperature of 45 ºC and pressure of 50 bar.

3.6. Structural characterization post-adsorption and desorption process of MOF-808-AC

Through the FTIR analysis of the MOF-808-AC, as seen in Figure 12, it is noted that the characteristic bands of the bonds formed by the synthesis are maintained and have similar intensity even after the analyses under high pressure, resulting then in a high chemical stability following treatment. Additionally, the analysis of the x-ray diffraction after the application under pressurized system is observed in Figure 13. Hence, it may be inferred that the MOF-808-AC sample maintains its crystallinity with the presence of the characteristic peaks at (8.35°), (8.75°), (10.0°) and (11.0°) as related to the crystalline framework of planes (311), (222), (400), and (331). It suggests these materials have a proper stability.

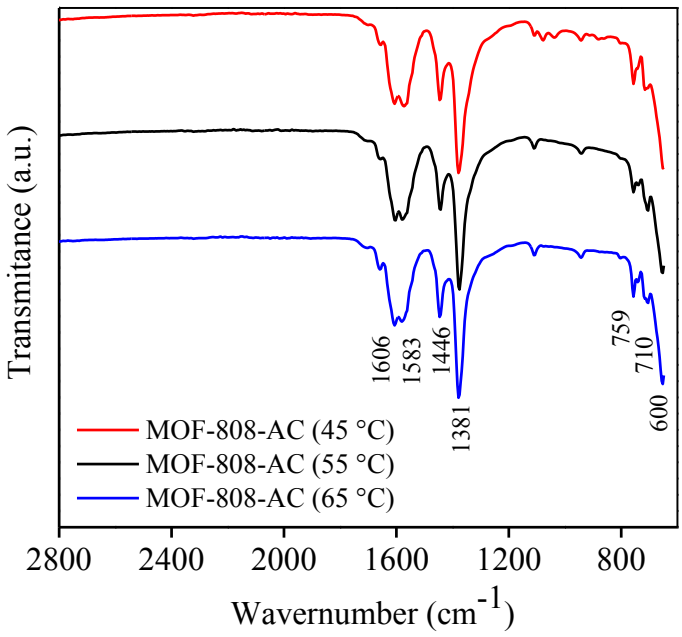

Figure 12. Infrared spectrum (FTIR) of the metal-organic framework MOF-808-AC after CO_2 adsorption and desorption isotherms between 1 and 50 bar at temperatures of 45 °C, 55 °C and 65 °C.

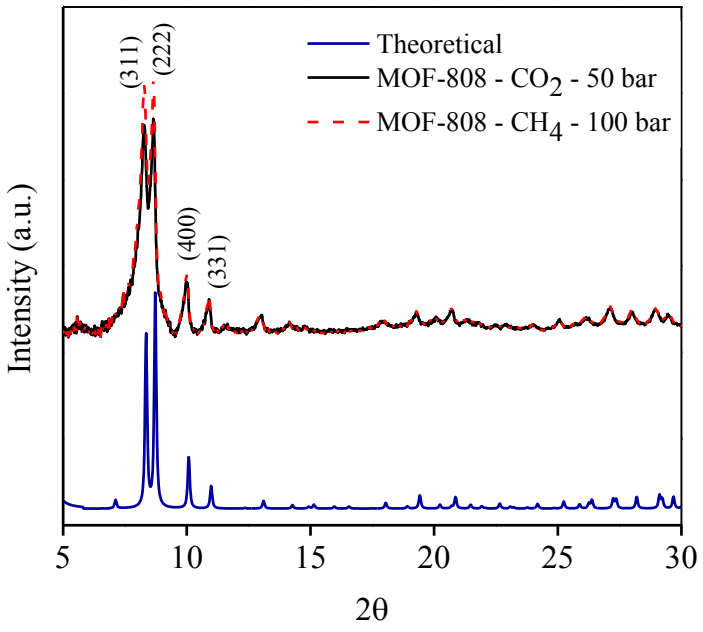

Figure 13. X-ray diffraction profile of MOF-808-AC after CO_2 and CH_4 adsorption and desorption isotherms at 45 °C and pressure of up to 100 bar.

3.7. Wet CO_2 adsorption

It is noteworthy that MOF-808-AC exhibits low N_2 adsorption capacity under dry conditions. Thus, the coadsorption of N_2 can be considered insignificant during multicomponent measurements involving CO_2 and H_2O.

The presence of 15 % humid CO_2 for MOF-808-AC resulted in an adsorbed quantity of approximately 14 g/100 g shown in Figure 14. Both investigations conducted by MILNER et al. (2017) [95] and CHOE et al. (2022) [96] report that metal-organic frameworks adsorb water and CO_2 at the same active sites, with water adsorption being more favorable. This proclivity typically culminates in the prevalence of water adsorption over CO_2 in multicomponent measurements. The hysteresis loop closes at approximately 100 °C for MOF-808-AC. Despite the presence of narrow micropores, the energy required for desorption remains relatively mild. It is worth emphasizing that the presence of a narrow loop in the metal-organic framework renders it a promising candidate for the adsorption and separation of humid CO_2 in diverse systems. This attribute is predicated on the ability to effectuate regeneration at mild temperatures, concurrently achieving an impressive yield exceeding 80 % of the MOF's adsorption capacity in subsequent cycles.

Furthermore, it can be noted that the lines from each cycle overlap, exhibiting adsorbed quantity values of 14 g/100 g for MOF-808-AC. This suggests that regeneration occurred efficiently, even at a mild temperature of 110 °C. This could be directly linked to the prevalent presence of physisorption processes, in which the interactions between gases and metal-organic frameworks are weaker. These findings imply that regeneration occurred efficiently, requiring lower temperatures and, consequently, reduced energy expenditure.

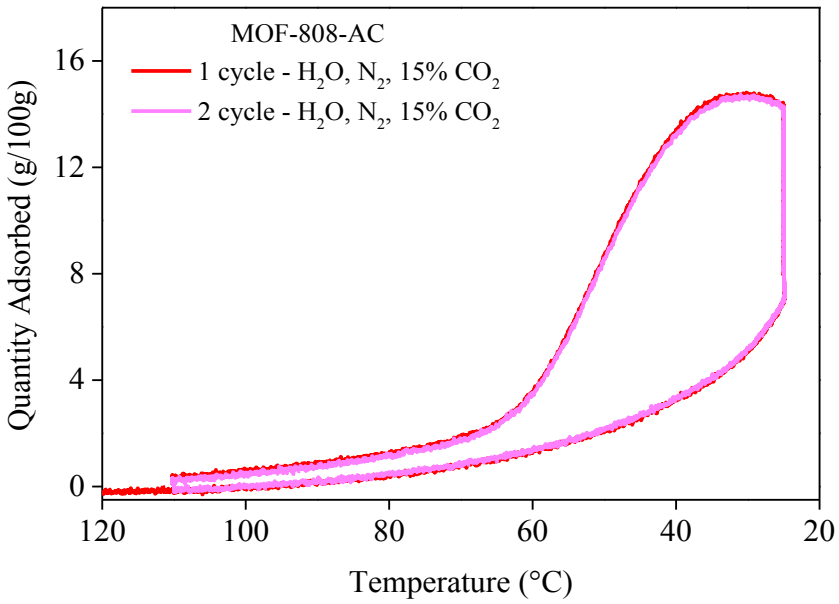

Figure 14. Two cycles of N_2, CO_2, and H_2O adsorption on the metal-organic framework MOF-808-AC.

Long-term stability is a critical factor in the selection of an adsorbent, especially in humid environments where there are few available reports in the literature. In Figure 15, it is evident that the adsorption capacity remained constant throughout the adsorption and desorption cycles, with no decrease in adsorption efficiency. This suggests good material stability. Furthermore, MOF-808-AC was efficiently regenerated at a temperature of 110 °C, obviating the necessity for vacuum or pressure differentials. This signifies that the regeneration process proves efficacious, thereby enhancing the practical viability of these adsorbents in real-world applications.

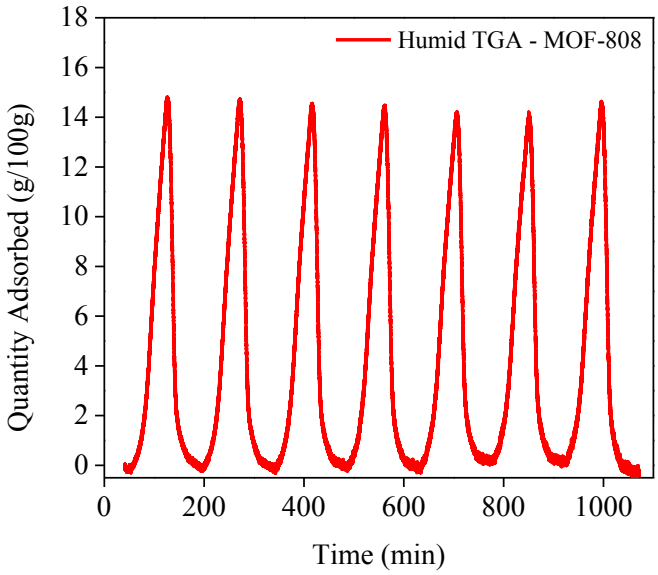

Figure 15. Adsorption and desorption cycles of N_2, CO_2, and H_2O on MOF-808-AC.

In order to elucidate the adsorption mechanism of humid CO_2, within the metal-organic framework MOF-808-AC, experiments employing ^{13}C nuclear magnetic resonance (NMR) spectroscopy were conducted. In the ^{13}C NMR spectrum attributed to MOF-808-AC (Figure 16), only one signal at δ 13C = 125 ppm was observed, indicating the presence of physisorbed CO_2 in the material. These outcomes align with antecedent investigations conducted by LYU et al. (2022), ETHIER et al. (2015) and MAO et al. (2022), which also identified this distinctive signal indicative of physisorbed CO_2 [48,97,98].

Therefore, the results demonstrate that even in the adsorption of humid CO_2, the MOF-808-AC exhibit solely physical interactions, thereby corroborating the previously hypothesis. These weaker interactions between the gases and the metal-organic frameworks engender a regenerative process of heightened efficacy, requiring milder temperatures (below 150 °C). This implies to a reduced energy expenditure compared to conventional adsorbents such as zeolites and silica gel, which typically necessitate temperatures ranging from 200 °C to 250 °C for regeneration.

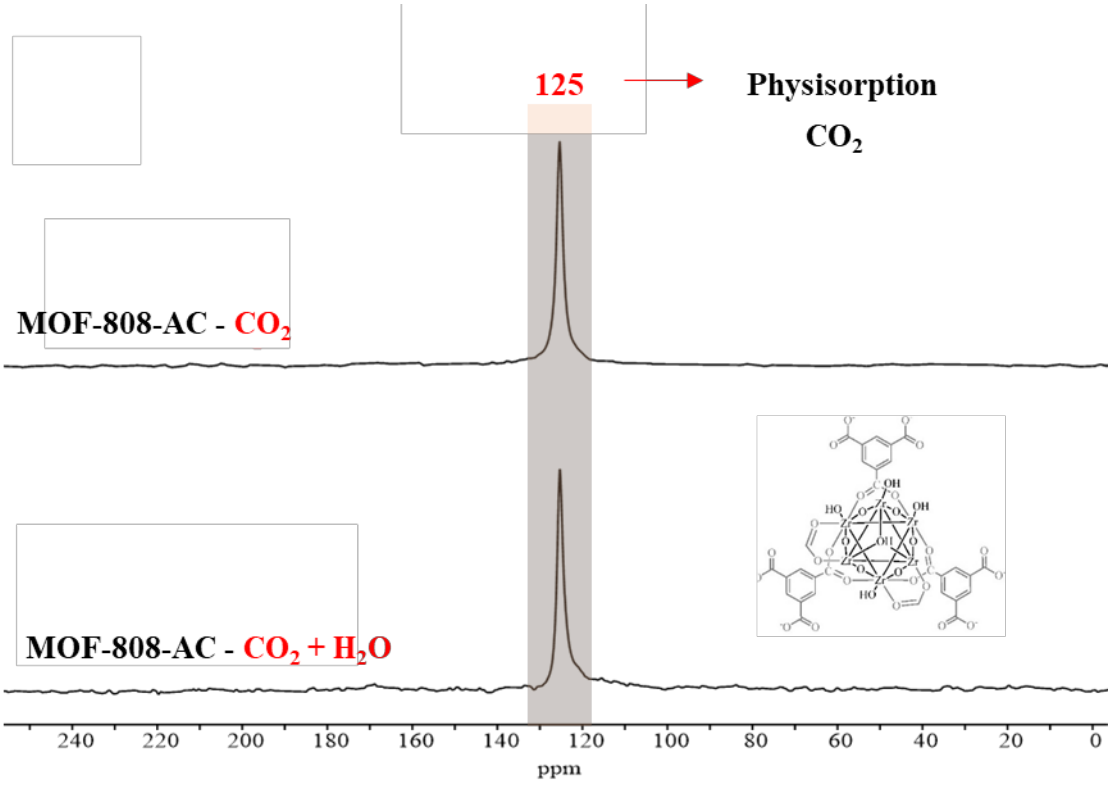

Figure 16. Espectros de 13C – ressonância magnética nuclear de estado sólido da estrutura MOF-808-AC pós adsorção de CO_2 com e sem presença de água.

4. Conclusion

The characterizations shown that MOF-808 synthesized in autoclave exhibited a higher surface area, a larger pore volume, and maintained its structural crystallinity characteristics with a reduced synthesis time compared to conventionally synthesized MOF-808, MOF-808-AC (1502 $m^2\ g^{-1}$ and 0.63 $cm^3\ g^{-1}$) and MOF-808-C (1323 $m^2\ g^{-1}$ and 0.51 $cm^3\ g^{-1}$). Additionally, the scanning electron microscopy analyses demonstrate the existence of particles with highly monodisperse morphologies and uniformly distributed. Thermogravimetric analysis revealed the presence of the solvent used in the pores of MOF-808-C, leading to a decrease in the surface area.

With the CO_2 and CH_4 adsorption analysis under a pressurized system, the low selectivity for the CH_4 molecules was identified and also the MOF-808-AC adsorbed a high amount of CO_2, 24.6

mmol g^{-1}. This value is superior to those found with the zeolites and silica gels being currently employed in most investigations. These values, in association with the selectivity of the adsorbent, point to an important potential towards separating CO_2 and CH_4 mixtures. Furthermore, the good stability of the material following 5 cycles of adsorption could be observed and it was possible to infer that the reaction between the CO_2 molecules and that of the MOF-808 is exothermic and the process is physical, it may contribute to reducing energy expenditure at industrial processing plants.

Finally, it was possible to infer that under the conditions of 15 % humid CO_2 in N_2, the adsorption capacity remained constant after continuous cycles of adsorption and desorption. Furthermore, it was also possible to demonstrate that regeneration occurred efficiently even at a mild temperature of 110 °C, which can result in energy savings in industrial processing plants. This mild regeneration temperature was explained by the presence of only physisorption processes, weak interactions, confirmed in the nuclear magnetic resonance analysis.

5. CRediT authorship contribution statement

Tamires R. Menezes: Writing - original draft and Formal analysis. **Kátilla M.C. Santos:** Writing - review & editing. **Haiyan Mao:** Writing - review & editing. **Klebson Santos:** Writing - review & editing. **Juliana F. De Conto:** Project administration and Supervision. **Jeffrey A. Reimer:** Supervision, review & editing. **Silvia M. E. Dariva:** Supervision, review & editing. **Cesar C. Santana1:** Supervision, review & editing.

6. Declaration of competing interest

The authors declare that they have no known competing financial interests or personal relationships that could have appeared to influence the work reported in this paper.

7. Acknowledgments

This study was financed, in part, by the CAPES (Coordination for the Improvement of Higher Education Personnel) - Finance Code 001, CNPq (National Council for Scientific and Technological Development) and PETROBRAS S.A (financial support and scholarships). All authors have read and agreed to the published version of the manuscript.

8. References

[1] W. Zhang, Y. Liu, S. Ren, R. Wang, Experimental characterizations and modeling of electrical resistance in hydrate bearing sediments, in: ICMREE2011 - Proceedings 2011 International Conference on Materials for Renewable Energy and Environment, 2011. https://doi.org/10.1109/ICMREE.2011.5930720.

[2] M.Z. Jacobson, The health and climate impacts of carbon capture and direct air capture, Energy Environ Sci 12 (2019). https://doi.org/10.1039/c9ee02709b.

[3] K.M.C. Santos, T.R. Menezes, M.R. Oliveira, T.S.L. Silva, K.S. Santos, V.A. Barros, D.C. Melo, A.L. Ramos, C.C. Santana, E. Franceschi, C. Dariva, S.M. Egues, G.R. Borges, J.F. De Conto, Natural gas dehydration by adsorption using MOFs and silicas: A review, Sep Purif Technol 276 (2021). https://doi.org/10.1016/j.seppur.2021.119409.

[4] X. Zhang, N. Huang, G. Wang, W. Dong, M. Yang, Y. Luan, Z. Shi, Synthesis of highly loaded and well dispersed CuO/SBA-15 via an ultrasonic post-grafting method and its application as a catalyst for the direct hydroxylation of benzene to phenol, Microporous and Mesoporous Materials 177 (2013). https://doi.org/10.1016/j.micromeso.2013.04.012.

[5] W. Huang, X. Zhou, Q. Xia, J. Peng, H. Wang, Z. Li, Preparation and adsorption performance of GrO@Cu-BTC for separation of CO2/CH4, Ind Eng Chem Res 53 (2014). https://doi.org/10.1021/ie501040s.

[6] P. Chowdhury, C. Bikkina, S. Gumma, Gas adsorption properties of the chromium-based metal organic framework MIL-101, Journal of Physical Chemistry C 113 (2009). https://doi.org/10.1021/jp811418r.

[7] L. Mafra, T. Čendak, S. Schneider, P. V. Wiper, J. Pires, J.R.B. Gomes, M.L. Pinto, Amine functionalized porous silica for CO2/CH4 separation by adsorption: Which amine and why, Chemical Engineering Journal 336 (2018). https://doi.org/10.1016/j.cej.2017.12.061.

[8] Q. Wu, X. Liu, L. Zhu, L. Ding, P. Gao, X. Wang, S. Pan, C. Bian, X. Meng, J. Xu, F. Deng, S. Maurer, U. Müller, F.S. Xiao, Solvent-free synthesis of zeolites from anhydrous starting raw solids, J Am Chem Soc 137 (2015). https://doi.org/10.1021/ja5124013.

[9] M. Sinaei Nobandegani, L. Yu, J. Hedlund, Zeolite membrane process for industrial CO2/CH4 separation, Chemical Engineering Journal 446 (2022). https://doi.org/10.1016/j.cej.2022.137223.

[10] T. Yu, Q. Cai, G. Lian, Y. Bai, X. Zhang, X. Zhang, L. Liu, S. Zhang, Mechanisms behind high CO2/CH4 selectivity using ZIF-8 metal organic frameworks with encapsulated ionic liquids: A computational study, Chemical Engineering Journal 419 (2021). https://doi.org/10.1016/j.cej.2021.129638.

[11] S.A. Abdollahi, A.R. Andarkhor, A. Pourahmad, A.H. Alibak, F. Alobaid, B. Aghel, Simulating and Comparing CO2/CH4 Separation Performance of Membrane–Zeolite Contactors by Cascade Neural Networks, Membranes (Basel) 13 (2023). https://doi.org/10.3390/membranes13050526.

[12] N. Singh, S. Dalakoti, A. Sharma, R. Chauhan, R.S. Murali, S. Divekar, S. Dasgupta, Aarti, Shaping of MIL-53-Al and MIL-101 MOF for CO2/CH4, CO2/N2 and CH4/N2 separation, Sep Purif Technol 341 (2024). https://doi.org/10.1016/j.seppur.2024.126820.

[13] M. Yahia, L.A. Lozano, J.M. Zamaro, C. Téllez, J. Coronas, Microwave-assisted synthesis of metal–organic frameworks UiO-66 and MOF-808 for enhanced CO2/CH4 separation in PIM-1 mixed matrix membranes, Sep Purif Technol 330 (2024). https://doi.org/10.1016/j.seppur.2023.125558.

[14] B. Liu, B. Smit, Molecular simulation studies of separation of CO2/N2, CO2/CH4, and CH4/N2 by ZIFs, Journal of Physical Chemistry C 114 (2010). https://doi.org/10.1021/jp101531m.

[15] T. Menezes, K. Santos, E. Franceschi, G. Borges, C. Dariva, S. Egues, J. De Conto, C. Santana, Synthesis of the chiral stationary phase based on functionalized ZIF-8 with amylose carbamate, J Mater Res 35 (2020). https://doi.org/10.1557/jmr.2020.276.

[16] O.M. Yaghi, G. Li, H. Li, Selective binding and removal of guests in a microporous metal–organic framework, Nature 378 (1995). https://doi.org/10.1038/378703a0.

[17] Y. Fu, Y. Yao, A.C. Forse, J. Li, K. Mochizuki, J.R. Long, J.A. Reimer, G. De Paëpe, X. Kong, Solvent-derived defects suppress adsorption in MOF-74, Nat Commun 14 (2023). https://doi.org/10.1038/s41467-023-38155-8.

[18] P.G. Boyd, A. Chidambaram, E. García-Díez, C.P. Ireland, T.D. Daff, R. Bounds, A. Gładysiak, P. Schouwink, S.M. Moosavi, M.M. Maroto-Valer, J.A. Reimer, J.A.R. Navarro, T.K. Woo, S. Garcia, K.C. Stylianou, B. Smit, Data-driven design of metal–organic frameworks for wet flue gas CO2 capture, Nature 576 (2019). https://doi.org/10.1038/s41586-019-1798-7.

[19] H. Daglar, S. Aydin, S. Keskin, MOF-based MMMs breaking the upper bounds of polymers for a large variety of gas separations, Sep Purif Technol 281 (2022). https://doi.org/10.1016/j.seppur.2021.119811.

[20] D. Alezi, Y. Belmabkhout, M. Suyetin, P.M. Bhatt, L.J. Weseliński, V. Solovyeva, K. Adil, I. Spanopoulos, P.N. Trikalitis, A.H. Emwas, M. Eddaoudi, MOF Crystal Chemistry Paving

the Way to Gas Storage Needs: Aluminum-Based soc -MOF for CH4, O2, and CO2 Storage, J Am Chem Soc 137 (2015). https://doi.org/10.1021/jacs.5b07053.

[21] W. Fan, Y. Ying, S.B. Peh, H. Yuan, Z. Yang, Y. Di Yuan, D. Shi, X. Yu, C. Kang, D. Zhao, Multivariate Polycrystalline Metal-Organic Framework Membranes for CO2/CH4Separation, J Am Chem Soc 143 (2021). https://doi.org/10.1021/jacs.1c08404.

[22] R. Wei, T. Alshahrani, B. Chen, A.B. Ibragimov, H. Xu, J. Gao, Advances in porous materials for efficient separation and purification of flue gas, Sep Purif Technol 352 (2025) 128238. https://doi.org/10.1016/J.SEPPUR.2024.128238.

[23] X. Cen, Y. Sun, C. Yu, C. Geng, Z. Gu, D. Ao, Z. Zhang, Z. Qiao, C. Zhong, A facile synthesis of monolithic MOF single crystal for gas separation via a supersaturation strategy, Sep Purif Technol 334 (2024) 125995. https://doi.org/10.1016/J.SEPPUR.2023.125995.

[24] H.R. Liu, S.C. Liu, L.P. Zhang, Y.T. Li, X.M. Peng, J. Wang, Q.Y. Yang, Pore chemically modified nickel-based metal-organic frameworks for efficient purification of natural gas, Sep Purif Technol 352 (2025) 128267. https://doi.org/10.1016/J.SEPPUR.2024.128267.

[25] T. Rodenas, M. Van Dalen, E. García-Pérez, P. Serra-Crespo, B. Zornoza, F. Kapteijn, J. Gascon, Visualizing MOF mixed matrix membranes at the nanoscale: Towards structure-performance relationships in CO2/CH4 separation over NH2-MIL-53(Al)@PI, Adv Funct Mater 24 (2014). https://doi.org/10.1002/adfm.201203462.

[26] M.T. Kallo, M.J. Lennox, Understanding CO2/CH4Separation in Pristine and Defective 2D MOF CuBDC Nanosheets via Nonequilibrium Molecular Dynamics, Langmuir 36 (2020). https://doi.org/10.1021/acs.langmuir.0c02434.

[27] H. Zhu, W. Wang, Y. Huo, X. He, H. Zhao, H. Wang, Molecular Simulation Study on Adsorption and Diffusion Behaviors of CO2/N2in Lignite, ACS Omega 5 (2020). https://doi.org/10.1021/acsomega.0c04352.

[28] H. Wang, M. Wang, X. Liang, J. Yuan, H. Yang, S. Wang, Y. Ren, H. Wu, F. Pan, Z. Jiang, Organic molecular sieve membranes for chemical separations, Chem Soc Rev 50 (2021). https://doi.org/10.1039/d0cs01347a.

[29] M.Z. Ahmad, T.A. Peters, N.M. Konnertz, T. Visser, C. Téllez, J. Coronas, V. Fila, W.M. de Vos, N.E. Benes, High-pressure CO2/CH4 separation of Zr-MOFs based mixed matrix membranes, Sep Purif Technol 230 (2020). https://doi.org/10.1016/j.seppur.2019.115858.

[30] A. Mousavinejad, A. Rahimpour, M.R. Shirzad Kebria, S. Khoshhal Salestan, M. Sadrzadeh, N. Tavajohi Hassan Kiadeh, Nickel-Based Metal-Organic Frameworks to Improve the CO2/CH4Separation Capability of Thin-Film Pebax Membranes, Ind Eng Chem Res 59 (2020). https://doi.org/10.1021/acs.iecr.0c01017.

[31] C. Jiao, X. Song, X. Zhang, L. Sun, H. Jiang, MOF-Mediated Interfacial Polymerization to Fabricate Polyamide Membranes with a Homogeneous Nanoscale Striped Turing Structure for CO2/CH4Separation, ACS Appl Mater Interfaces 13 (2021). https://doi.org/10.1021/acsami.1c03737.

[32] P. Küsgens, M. Rose, I. Senkovska, H. Fröde, A. Henschel, S. Siegle, S. Kaskel, Characterization of metal-organic frameworks by water adsorption, Microporous and Mesoporous Materials 120 (2009). https://doi.org/10.1016/j.micromeso.2008.11.020.

[33] A. Domán, O. Czakkel, L. Porcar, J. Madarász, E. Geissler, K. László, Role of water molecules in the decomposition of HKUST-1: Evidence from adsorption, thermoanalytical, X-ray and neutron scattering measurements, Appl Surf Sci 480 (2019). https://doi.org/10.1016/j.apsusc.2019.02.177.

[34] J.A. Greathouse, M.D. Allendorf, The interaction of water with MOF-5 simulated by molecular dynamics, J Am Chem Soc 128 (2006). https://doi.org/10.1021/ja063506b.

[35] K. Schröck, F. Schröder, M. Heyden, R.A. Fischer, M. Havenith, Characterization of interfacial water in MOF-5 (Zn4(O)(BDC) 3)-a combined spectroscopic and theoretical study, Physical Chemistry Chemical Physics 10 (2008). https://doi.org/10.1039/b807458p.

[36] Y. Ming, J. Purewal, J. Yang, C. Xu, R. Soltis, J. Warner, M. Veenstra, M. Gaab, U. Müller, D.J. Siegel, Kinetic stability of MOF-5 in humid environments: Impact of powder densification, humidity level, and exposure time, Langmuir 31 (2015). https://doi.org/10.1021/acs.langmuir.5b00833.

[37] S. Zuluaga, E.M.A. Fuentes-Fernandez, K. Tan, F. Xu, J. Li, Y.J. Chabal, T. Thonhauser, Understanding and controlling water stability of MOF-74, J Mater Chem A Mater 4 (2016). https://doi.org/10.1039/c5ta10416e.

[38] L. Wang, X. Li, B. Yang, K. Xiao, H. Duan, H. Zhao, The chemical stability of metal-organic frameworks in water treatments: Fundamentals, effect of water matrix and judging methods, Chemical Engineering Journal 450 (2022). https://doi.org/10.1016/j.cej.2022.138215.

[39] T.B. Čelič, A. Škrjanc, J.M. Coronado, T. Čendak, V.A. de la Peña O'Shea, D.P. Serrano, N. Zabukovec Logar, New Insight into Sorption Cycling Stability of Three Al-Based MOF Materials in Water Vapour, Nanomaterials 12 (2022). https://doi.org/10.3390/nano12122092.

[40] X. Ma, J. Tan, Z. Li, D. Huang, S. Xue, Y. Xu, H. Tao, Fabrication of Stable MIL-53(Al) for Excellent Removal of Rhodamine B, Langmuir 38 (2022). https://doi.org/10.1021/acs.langmuir.1c02836.

[41] C. Férey, C. Mellot-Draznieks, C. Serre, F. Millange, J. Dutour, S. Surblé, I. Margiolaki, Chemistry: A chromium terephthalate-based solid with unusually large pore volumes and surface area, Science (1979) 309 (2005). https://doi.org/10.1126/science.1116275.

[42] S. Fei, A. Alizadeh, W.L. Hsu, J.J. Delaunay, H. Daiguji, Analysis of the Water Adsorption Mechanism in Metal-Organic Framework MIL-101(Cr) by Molecular Simulations, Journal of Physical Chemistry C 125 (2021). https://doi.org/10.1021/acs.jpcc.1c06917.

[43] A. Schaate, P. Roy, A. Godt, J. Lippke, F. Waltz, M. Wiebcke, P. Behrens, Modulated synthesis of Zr-based metal-organic frameworks: From nano to single crystals, Chemistry - A European Journal 17 (2011). https://doi.org/10.1002/chem.201003211.

[44] J.H. Cavka, S. Jakobsen, U. Olsbye, N. Guillou, C. Lamberti, S. Bordiga, K.P. Lillerud, A new zirconium inorganic building brick forming metal organic frameworks with exceptional stability, J Am Chem Soc 130 (2008). https://doi.org/10.1021/ja8057953.

[45] S. Krause, V. Bon, U. Stoeck, I. Senkovska, D.M. Többens, D. Wallacher, S. Kaskel, A Stimuli-Responsive Zirconium Metal–Organic Framework Based on Supermolecular Design, Angewandte Chemie - International Edition 56 (2017). https://doi.org/10.1002/anie.201702357.

[46] D. Feng, K. Wang, J. Su, T.F. Liu, J. Park, Z. Wei, M. Bosch, A. Yakovenko, X. Zou, H.C. Zhou, A highly stable zeotype mesoporous zirconium metal-organic framework with ultralarge pores, Angewandte Chemie - International Edition 54 (2015). https://doi.org/10.1002/anie.201409334.

[47] J.M. Park, D.K. Yoo, S.H. Jhung, Selective CO2 adsorption over functionalized Zr-based metal organic framework under atmospheric or lower pressure: Contribution of functional groups to adsorption, Chemical Engineering Journal 402 (2020). https://doi.org/10.1016/j.cej.2020.126254.

[48] H. Lyu, O.I.F. Chen, N. Hanikel, M.I. Hossain, R.W. Flaig, X. Pei, A. Amin, M.D. Doherty, R.K. Impastato, T.G. Glover, D.R. Moore, O.M. Yaghi, Carbon Dioxide Capture Chemistry of Amino Acid Functionalized Metal-Organic Frameworks in Humid Flue Gas, J Am Chem Soc 144 (2022). https://doi.org/10.1021/jacs.1c13368.

[49] H.J. Jun, D.K. Yoo, S.H. Jhung, Metal-organic framework (MOF-808) functionalized with ethyleneamines: Selective adsorbent to capture CO2under low pressure, Journal of CO2 Utilization 58 (2022). https://doi.org/10.1016/j.jcou.2022.101932.

[50] J. Duan, M. Higuchi, S. Horike, M.L. Foo, K.P. Rao, Y. Inubushi, T. Fukushima, S. Kitagawa, High CO2/CH4 and C2 hydrocarbons/CH4 selectivity in a chemically robust porous coordination polymer, Adv Funct Mater 23 (2013). https://doi.org/10.1002/adfm.201203288.

[51] L. Qin, Y. Li, F. Liang, L. Li, Y. Lan, Z. Li, X. Lu, M. Yang, D. Ma, A microporous 2D cobalt-based MOF with pyridyl sites and open metal sites for selective adsorption of CO2, Microporous and Mesoporous Materials 341 (2022). https://doi.org/10.1016/j.micromeso.2022.112098.

[52] S. Couck, J.F.M. Denayer, G. V. Baron, T. Rémy, J. Gascon, F. Kapteijn, An amine-functionalized MIL-53 metal-organic framework with large separation power for CO2 and CH4, J Am Chem Soc 131 (2009). https://doi.org/10.1021/ja900555r.

[53] M. Gheytanzadeh, A. Baghban, S. Habibzadeh, A. Esmaeili, O. Abida, A. Mohaddespour, M.T. Munir, Towards estimation of CO2 adsorption on highly porous MOF-based adsorbents using gaussian process regression approach, Sci Rep 11 (2021). https://doi.org/10.1038/s41598-021-95246-6.

[54] H. Furukawa, F. Gándara, Y.B. Zhang, J. Jiang, W.L. Queen, M.R. Hudson, O.M. Yaghi, Water adsorption in porous metal-organic frameworks and related materials, J Am Chem Soc 136 (2014). https://doi.org/10.1021/ja500330a.

[55] J.E. Efome, D. Rana, T. Matsuura, C.Q. Lan, Effects of operating parameters and coexisting ions on the efficiency of heavy metal ions removal by nano-fibrous metal-organic framework membrane filtration process, Science of the Total Environment 674 (2019). https://doi.org/10.1016/j.scitotenv.2019.04.187.

[56] W. Jumpathong, T. Pila, Y. Lekjing, P. Chirawatkul, B. Boekfa, S. Horike, K. Kongpatpanich, Exploitation of missing linker in Zr-based metal-organic framework as the catalyst support for selective oxidation of benzyl alcohol, APL Mater 7 (2019). https://doi.org/10.1063/1.5126077.

[57] S. Van Der Walt, J.L. Schönberger, J. Nunez-Iglesias, F. Boulogne, J.D. Warner, N. Yager, E. Gouillart, T. Yu, Scikit-image: Image processing in python, PeerJ 2014 (2014). https://doi.org/10.7717/peerj.453.

[58] R. Kober, M. Schwaab, E. Steffani, E. Barbosa-Coutinho, J.C. Pinto, A.L. Alberton, D-optimal experimental designs for precise parameter estimation of adsorption equilibrium models, Chemometrics and Intelligent Laboratory Systems 192 (2019). https://doi.org/10.1016/j.chemolab.2019.103823.

[59] Q. Liu, Q. Zhang, B. Liu, J. Ma, A new synthesis and adsorption mechanism of ZrO2 based metal-organic frames for efficient removal of mercury ions from aqueous solution, Ceram Int 45 (2019). https://doi.org/10.1016/j.ceramint.2019.04.246.

[60] K. Xuan, Y. Pu, F. Li, J. Luo, N. Zhao, F. Xiao, Metal-organic frameworks MOF-808-X as highly efficient catalysts for direct synthesis of dimethyl carbonate from CO2 and methanol, Chinese Journal of Catalysis 40 (2019). https://doi.org/10.1016/S1872-2067(19)63291-2.

[61] W. Zhang, A. Bu, Q. Ji, L. Min, S. Zhao, Y. Wang, J. Chen, P Ka-directed incorporation of phosphonates into mof-808 via ligand exchange: Stability and adsorption properties for uranium, ACS Appl Mater Interfaces 11 (2019). https://doi.org/10.1021/acsami.9b10920.

[62] M.W. Logan, S. Langevin, Z. Xia, Reversible Atmospheric Water Harvesting Using Metal-Organic Frameworks, Sci Rep 10 (2020). https://doi.org/10.1038/s41598-020-58405-9.

[63] F.G. Cirujano, N. Martín, G. Fu, C. Jia, D. De Vos, Cooperative acid-base bifunctional ordered porous solids in sequential multi-step reactions: MOF: vs. mesoporous silica, Catal Sci Technol 10 (2020). https://doi.org/10.1039/c9cy02404b.

[64] Y. Gu, G. Ye, W. Xu, W. Zhou, Y. Sun, Creation of Active Sites in MOF-808(Zr) by a Facile Route for Oxidative Desulfurization of Model Diesel Oil, ChemistrySelect 5 (2020). https://doi.org/10.1002/slct.201903376.

[65] S. Lin, Y. Zhao, Y.S. Yun, Highly Effective Removal of Nonsteroidal Anti-inflammatory Pharmaceuticals from Water by Zr(IV)-Based Metal-Organic Framework: Adsorption Performance and Mechanisms, ACS Appl Mater Interfaces 10 (2018). https://doi.org/10.1021/acsami.8b08596.

[66] H. Liu, Z. Zhang, J. Tang, Z. Fei, Q. Liu, X. Chen, M. Cui, X. Qiao, Quest for pore size effect on the catalytic property of defect-engineered MOF-808-SO4 in the addition

reaction of isobutylene with ethylene glycol, J Solid State Chem 269 (2019). https://doi.org/10.1016/j.jssc.2018.07.030.

[67] C. Ji, Y. Ren, H. Yu, M. Hua, L. Lv, W. Zhang, Highly efficient and selective Hg(II) removal from water by thiol-functionalized MOF-808: Kinetic and mechanism study, Chemical Engineering Journal 430 (2022). https://doi.org/10.1016/j.cej.2021.132960.

[68] Y. Kalinovskyy, N.J. Cooper, M.J. Main, S.J. Holder, B.A. Blight, Microwave-assisted activation and modulator removal in zirconium MOFs for buffer-free CWA hydrolysis, Dalton Transactions 46 (2017). https://doi.org/10.1039/c7dt03616g.

[69] J. Xu, J. Liu, Z. Li, X. Wang, Y. Xu, S. Chen, Z. Wang, Optimized synthesis of Zr(iv) metal organic frameworks (MOFs-808) for efficient hydrogen storage, New Journal of Chemistry 43 (2019). https://doi.org/10.1039/C8NJ06362A.

[70] H. Bin Luo, Q. Ren, P. Wang, J. Zhang, L. Wang, X.M. Ren, High Proton Conductivity Achieved by Encapsulation of Imidazole Molecules into Proton-Conducting MOF-808, ACS Appl Mater Interfaces 11 (2019). https://doi.org/10.1021/acsami.9b01075.

[71] J. Jiang, F. Gándara, Y.B. Zhang, K. Na, O.M. Yaghi, W.G. Klemperer, Superacidity in sulfated metal-organic framework-808, J Am Chem Soc 136 (2014). https://doi.org/10.1021/ja507119n.

[72] K. Tan, S. Jensen, L. Feng, H. Wang, S. Yuan, M. Ferreri, J.P. Klesko, R. Rahman, J. Cure, J. Li, H.C. Zhou, T. Thonhauser, Y.J. Chabal, Reactivity of Atomic Layer Deposition Precursors with OH/H 2 O-Containing Metal Organic Framework Materials, Chemistry of Materials 31 (2019). https://doi.org/10.1021/acs.chemmater.8b01844.

[73] F.M. Valadi, S. Shahsavari, E. Akbarzadeh, M.R. Gholami, Preparation of new MOF-808/chitosan composite for Cr(VI) adsorption from aqueous solution: Experimental and DFT study, Carbohydr Polym 288 (2022). https://doi.org/10.1016/j.carbpol.2022.119383.

[74] K. Pirzadeh, A.A. Ghoreyshi, S. Rohani, M. Rahimnejad, Strong Influence of Amine Grafting on MIL-101 (Cr) Metal-Organic Framework with Exceptional CO2/N2 Selectivity, Ind Eng Chem Res 59 (2020). https://doi.org/10.1021/acs.iecr.9b05779.

[75] W. Lu, D. Yuan, J. Sculley, D. Zhao, R. Krishna, H.-C. Zhou, Sulfonate-Grafted Porous Polymer Networks for Preferential CO 2 Adsorption at Low Pressure, J. Am. Chem. Soc 133 (2011) 18126–18129. https://doi.org/10.1021/ja2087773.

[76] C. Guan, S. Liu, C. Li, Y. Wang, Y. Zhao, The temperature effect on the methane and CO2 adsorption capacities of Illinois coal, Fuel 211 (2018). https://doi.org/10.1016/j.fuel.2017.09.046.

[77] C.A. Grande, D.G.B. Morence, A.M. Bouzga, K.A. Andreassen, Silica Gel as a Selective Adsorbent for Biogas Drying and Upgrading, Ind Eng Chem Res 59 (2020). https://doi.org/10.1021/acs.iecr.0c00949.

[78] J.A. Cecilia, E. Vilarrasa-García, R. Morales-Ospino, M. Bastos-Neto, D.C.S. Azevedo, E. Rodríguez-Castellón, Insights into CO2 adsorption in amino-functionalized SBA-15

synthesized at different aging temperature, Adsorption 26 (2020). https://doi.org/10.1007/s10450-019-00118-1.

[79] V. Garshasbi, M. Jahangiri, M. Anbia, Equilibrium CO 2 adsorption on zeolite 13X prepared from natural clays, Appl Surf Sci 393 (2017). https://doi.org/10.1016/j.apsusc.2016.09.161.

[80] A. Bakhtyari, M. Mofarahi, C.H. Lee, CO2 adsorption by conventional and nanosized zeolites, in: Advances in Carbon Capture: Methods, Technologies and Applications, 2020. https://doi.org/10.1016/B978-0-12-819657-1.00009-8.

[81] S. Himeno, T. Komatsu, S. Fujita, High-pressure adsorption equilibria of methane and carbon dioxide on several activated carbons, J Chem Eng Data 50 (2005). https://doi.org/10.1021/je049786x.

[82] S.K. Wahono, J. Stalin, J. Addai-Mensah, W. Skinner, A. Vinu, K. Vasilev, Physico-chemical modification of natural mordenite-clinoptilolite zeolites and their enhanced CO2 adsorption capacity, Microporous and Mesoporous Materials 294 (2020). https://doi.org/10.1016/j.micromeso.2019.109871.

[83] H.G.T. Nguyen, L. Espinal, R.D. van Zee, M. Thommes, B. Toman, M.S.L. Hudson, E. Mangano, S. Brandani, D.P. Broom, M.J. Benham, K. Cychosz, P. Bertier, F. Yang, B.M. Krooss, R.L. Siegelman, M. Hakuman, K. Nakai, A.D. Ebner, L. Erden, J.A. Ritter, A. Moran, O. Talu, Y. Huang, K.S. Walton, P. Billemont, G. De Weireld, A reference high-pressure CO2 adsorption isotherm for ammonium ZSM-5 zeolite: results of an interlaboratory study, Adsorption 24 (2018). https://doi.org/10.1007/s10450-018-9958-x.

[84] L.H. De Oliveira, M. V. Pereira, J.G. Meneguin, M.A.S.D. De Barros, J.F. Do Nascimento, P.A. Arroyo, Influence of regeneration conditions on cyclic CO2adsorption on NaA zeolite at high pressures, Journal of CO2 Utilization 67 (2023). https://doi.org/10.1016/j.jcou.2022.102296.

[85] A.R. Millward, O.M. Yaghi, Metal-organic frameworks with exceptionally high capacity for storage of carbon dioxide at room temperature, J Am Chem Soc 127 (2005). https://doi.org/10.1021/ja0570032.

[86] M. Abunowara, M.A. Bustam, S. Sufian, M. Babar, U. Eldemerdash, A. Mukhtar, S. Ullah, M.A. Assiri, A.G. Al-Sehemi, S.S. Lam, High pressure CO2 adsorption onto Malaysian Mukah-Balingian coals: Adsorption isotherms, thermodynamic and kinetic investigations, Environ Res 218 (2023). https://doi.org/10.1016/j.envres.2022.114905.

[87] S. Salehi, M. Hosseinifard, Evaluation of CO2 and CH4 adsorption using a novel amine modified MIL-101-derived nanoporous carbon/polysaccharides nanocomposites: Isotherms and thermodynamics, Chemical Engineering Journal 410 (2021). https://doi.org/10.1016/j.cej.2020.128315.

[88] V.T. Ky, D.T. Quang, Mg2+ embedded MIL-101(Cr)-NH2 framework for improved CO2 adsorption and CO2/N2 selectivity, Vietnam Journal of Chemistry 59 (2021). https://doi.org/10.1002/vjch.202100035.

[89] J.J. Zhou, K.Y. Liu, C.L. Kong, L. Chen, Acetate-assisted synthesis of chromium(III) terephthalate and its gas adsorption properties, Bull Korean Chem Soc 34 (2013). https://doi.org/10.5012/bkcs.2013.34.6.1625.

[90] P. dos S. Gaschi, J.G. Meneguin, E.A. da Silva, A.L. Moretti, P.A. Arroyo, AVALIAÇÃO DE MÉTODOS DE CÁLCULO PARA O CALOR ISOSTÉRICO DE ADSORÇÃO DE CO2 E CH4 EM CARVÃO ATIVADO, in: 2018. https://doi.org/10.5151/cobeq2018-co.087.

[91] J.H. Lee, D.H. Suh, Entropy, enthalpy, and gibbs free energy variations of 133Cs via CO2-activated carbon filter and ferric ferrocyanide hybrid composites, Nuclear Engineering and Technology 53 (2021). https://doi.org/10.1016/j.net.2021.06.006.

[92] H. Ramezanipour Penchah, A. Ghaemi, H. Ghanadzadeh Gilani, Efficiency increase in hypercrosslinked polymer based on polystyrene in CO2 adsorption process, Polymer Bulletin 79 (2022). https://doi.org/10.1007/s00289-021-03678-x.

[93] N. Ayawei, A.N. Ebelegi, D. Wankasi, Modelling and Interpretation of Adsorption Isotherms, J Chem 2017 (2017). https://doi.org/10.1155/2017/3039817.

[94] S. Candamano, A. Policicchio, G. Conte, R. Abarca, C. Algieri, S. Chakraborty, S. Curcio, V. Calabrò, F. Crea, R.G. Agostino, Preparation of foamed and unfoamed geopolymer/NaX zeolite/activated carbon composites for CO2 adsorption, J Clean Prod 330 (2022). https://doi.org/10.1016/j.jclepro.2021.129843.

[95] P.J. Milner, R.L. Siegelman, A.C. Forse, M.I. Gonzalez, T. Runčevski, J.D. Martell, J.A. Reimer, J.R. Long, A Diaminopropane-Appended Metal-Organic Framework Enabling Efficient CO2 Capture from Coal Flue Gas via a Mixed Adsorption Mechanism, J Am Chem Soc 139 (2017). https://doi.org/10.1021/jacs.7b07612.

[96] J.H. Choe, H. Kim, M. Kang, H. Yun, S.Y. Kim, S.M. Lee, C.S. Hong, Functionalization of Diamine-Appended MOF-Based Adsorbents by Ring Opening of Epoxide: Long-Term Stability and CO2Recyclability under Humid Conditions, J Am Chem Soc 144 (2022). https://doi.org/10.1021/jacs.2c01488.

[97] A.L. Ethier, J.R. Switzer, A.C. Rumple, W. Medina-Ramos, Z. Li, J. Fisk, B. Holden, L. Gelbaum, P. Pollet, C.A. Eckert, C.L. Liotta, The effects of solvent and added bases on the protection of benzylamines with carbon dioxide, Processes 3 (2015). https://doi.org/10.3390/pr3030497.

[98] H. Mao, J. Tang, G.S. Day, Y. Peng, H. Wang, X. Xiao, Y. Yang, Y. Jiang, S. Chen, D.M. Halat, A. Lund, X. Lv, W. Zhang, C. Yang, Z. Lin, H.C. Zhou, A. Pines, Y. Cui, J.A. Reimer, A scalable solid-state nanoporous network with atomic-level interaction design for carbon dioxide capture, Sci Adv 8 (2022). https://doi.org/10.1126/sciadv.abo6849.

Declaration of interests

☒ The authors declare that they have no known competing financial interests or personal relationships that could have appeared to influence the work reported in this paper.

☐The authors declare the following financial interests/personal relationships which may be considered as potential competing interests: